The Journal of Green Energy and Environmental Engineering

Review Paper

Research Progress on Metal-Organic Frameworks as Drug Carriers

Dipanwita Raut[1], David Park[2,*]

[1] Department of Chemistry, Institute of Chemical Technology, Matunga, Mumbai 400019, India
[2] Center for Reticular Chemistry at California NanoSystems Institute, Department of Chemistry and Biochemistry, University of California, Los Angeles, CA 90095-1569, USA
*Corresponding author: D.Park@chem.ucla.edu

Abstract. Metal–organic frameworks (MOFs) are crystalline hybrids in which metal nodes or clusters are stitched into ordered nets by multitopic organic linkers. Their crystalline lattices combine ultra-large surface areas, mesoporous channels and engineerable metrics, while their room-temperature or solvothermal syntheses are remarkably straightforward. These features have propelled MOFs to the forefront of drug-delivery research, yet residual metal leaching and ligand degradation still raise cytotoxic red flags. Cyclodextrin-based MOFs (CD-MOFs)—built only from γ-cyclodextrin rings and biogenic K^+ ions—have recently been shown to bypass this bottleneck, offering an intrinsically benign, biocompatible platform for pharmaceutical applications. They can address the practical application shortcomings of MOFs in drug delivery, effectively improve the stability of guest drug molecules, and enhance efficacy, making them highly potential drug carriers. This article will review the synthesis and safety of CD-MOFs, as well as their advantages and limitations as drug carriers.

Keywords: *Metal-organic frameworks; Drug Carrier; research*

Received on 02 April 2024, Accepted on 28 June 2024, Published on 15 July 2024

1 Introduction

In modern society, the incidence and mortality rates of Alzheimer's disease (AD) and cancer are gradually increasing. Worldwide, AD and cancer are the seventh and second leading causes of death, respectively. Alzheimer's disease (AD) is a stealthily progressive neurodegenerative disorder that ranks as the leading trigger of dementia, combining prolonged pre-symptomatic latency with exceptionally high levels of both long-term disability and mortality. It is estimated that there are currently about 50 million AD patients worldwide. With the intensification of population aging, this number is expected to rapidly increase to more than double by 2050; if based on the biological (non-clinical) definition of AD, this estimated value would be three times higher [1, 2].Recent data show that 6 % of China's over-60 population are living with dementia; within this cohort, an estimated 15 million individuals are affected, and Alzheimer's disease accounts for more than 10 million of these cases. The main pathogenesis of AD includes β-amyloid protein (Aβ) plaque deposition, tau protein phosphorylation (p-tau) leading to neurofibrillary tangles, neuronal loss, and behavioral deficits such as memory and learning impairments [4, 5]. Recent studies have found that blood-brain barrier (BBB) damage, abnormal release of neurofilament light chain protein, gut microbiota imbalance, abnormal activation of pyroptosis, gene mutations, cholinergic system impairment, inflammation, microangiopathy, and metabolic disorders also play important roles in the pathogenesis of AD [6, 7]. Therapeutic strategies now target these pathways, and the FDA has licensed a trio of cholinesterase blockers—donepezil, rivastigmine, and galantamine—for routine clinical use. one N-methyl-D-aspartate receptor inhibitor—memantine; and their compound preparations (memantine and donepezil); two Aβ clearers—aducanumab and caninemab [8-10]. In addition, other drugs used to treat AD include calcium channel blockers, antioxidants, cerebral metabolic activators, 5-HT receptor antagonists, statins, and drugs regulating gut microbiota [11]. Although these drugs can alter the cognitive, behavioral, and functional

symptoms of AD, they can only delay the disease process and cannot cure or reverse the course of the disease. Moreover, long-term and large-scale drug use can lead to some side effects and adverse reactions, resulting in poor treatment outcomes for AD.

At the same time, the blood–brain barrier (BBB) remains a critical hurdle to effective therapy. Acting as a selective interface between the cerebral parenchyma and systemic blood (Fig. 1), this dynamic wall blocks the paracellular passage of most xenobiotics while tightly controlling nutrient flux to preserve CNS homeostasis [12,13]. Consequently, virtually all macromolecules and >98 % of small-molecule drugs are denied unrestricted entry into the brain. Therefore, to overcome the BBB, nanomaterial-mediated drug delivery systems (DDS) for targeted drug delivery to AD lesions have been extensively studied.

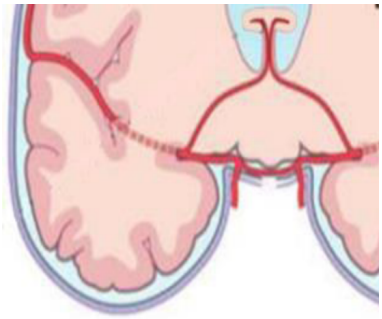

Figure 1 Schematic diagram of blood-brain barrier [14]

Cancer refers to malignant tumors originating from epithelial tissues. When the body is affected by carcinogenic substances in the environment (chemical, physical, viral, etc.) or due to factors such as genetics, endocrine, gender, and age, it leads to abnormal genetic changes, ultimately forming malignant tumors. Fresh IARC figures peg the planet's 2020 cancer toll at roughly 19.3 million new diagnoses and just under 10 million deaths; China alone contributed 4.57 million incident cases (≈ 24 % of the global total) and about 3 million fatalities (≈ 30 %), placing the country at the top of both rankings . It is projected that by 2030, the number of deaths due to cancer infections will reach 13.1 million [17, 18]. Currently, some drugs for treating cancer have been developed, such as doxorubicin hydrochloride, paclitaxel, and camptothecin. However, due to the presence of biological barriers, a large amount of the drug is lost, reducing the therapeutic effect. Increasing the dosage, in turn, enhances side effects. Therefore, to eliminate these limitations, measures need to be taken to improve the therapeutic effect of drugs, among which nano-drug delivery systems have received widespread attention. In short, engineering next-generation delivery platforms is pivotal to boosting clinical outcomes. Over the past decade, nanomaterials have surged forward, translating into major biomedical breakthroughs. Applying nanotechnology in the disease treatment process, encapsulating drugs in nano-drug delivery systems, and delivering them into the body via intravenous injection or oral administration. Shielded by nanocarriers, the cargo remains largely intact en route, translating into markedly improved therapeutic impact. Overall, nanomaterials hold exceptional promise for next-generation disease therapy.

2. Metal-Organic Framework Materials (MOFs)

2.1 Introduction to MOFs

Metal-organic framework materials, abbreviated as MOFs, are porous materials with periodic network structures formed by metal ions or metal ion clusters and organic ligands through coordination bonds [19]. As early as the 1980s, Robson et al. [20] discovered MOF materials. Subsequently, Yaghi et al. [21] first prepared MOF-5 ($Zn_4O(BDC)_3$) in 1995, which could maintain its framework structure after removing residual ligands or solvent molecules in the pores. Since then, researchers have continuously conducted studies and synthesized a large number of MOFs. Currently, most metals in the periodic table can be used as inorganic clusters to form MOFs, including the most common transition metals such as Zn, Cr, Cu, Fe, and lanthanide metals. Varying the metal node and linker pairing gives rise to distinct topological nets; this vast combinatorial space yields an ever-expanding library of MOF architectures. To date, over 20,000 MOF materials have been synthesized. It is worth

mentioning that according to materials genomics, over 400,000 MOF materials can be virtually constructed. Furthermore, compared to other types of porous materials, MOFs have shown good application prospects in constructing nano-drug delivery system platforms due to their high porosity, ease of functionalization, large specific surface area, and excellent biocompatibility. Studies have found that adding surfactants, crystallization regulators, etc., during the synthesis of MOFs can adjust the size and pore structure, thereby enabling MOFs to exhibit different structural properties, obtaining larger pore sizes or more defect sites [22, 23]. For instance, Li et al. [24] leveraged the zwitterionic surfactants CAPB and OAPB as structure-directing agents in water to grow Zr-based mesoporous MOFs that integrate ordered mesochannels with an intact microporous lattice, affording robust frameworks. In a separate approach, Cravillon et al. [25] tuned ZIF-8 dimensions from ~10 nm nanocrystals to ~1 μm microcrystals at ambient temperature by combining an excess of bidentate linker with a trio of crystallization suppressors—n-butylamine, 1-methylimidazole, and formate.

2.2 Classification of MOFs

There are many types of MOFs. Based on structural characteristics, topology, and the institutions of the preparers, multiple series of materials have been formed, such as IRMOF, ZIF, MIL, PCN, UiO, CPL, ZJU, and FJI. The structural characteristics and naming methods of common MOF materials are briefly introduced below.

2.2.1 ZIF Series (Zeolitic Imidazolate Frameworks)

The ZIF family (depicted in Fig. 1-2) was christened by Yaghi's team in the UC Berkeley chemistry department [26]. They are generally three-dimensional porous materials formed by the complexation of divalent transition metals (Zn^{2+}, Co^{2+}, Ni^{2+}) with imidazole or imidazole-derived organic ligands [27]. ZIF series materials have a structure similar to zeolite molecular sieves. In ZIFs, silicon and aluminum are swapped out for zinc or cobalt, while the oxygen bridges are supplanted by imidazole or its derivatives [28,29]. ZIF series materials have the advantages of large specific surface area, rich spatial structure, and high porosity. Compared with other MOFs, they also have good water stability, thermal stability, and chemical stability [30, 31]. Among the ZIF series materials, the most representative is ZIF-8. ZIF-8 assembles into a 3-D porous net that mimics sodalite's dodecahedral cage, stitched together by zinc nodes and imidazolate linkers via coordination bonds.In this structure, zinc ions and imidazolate structures are arranged alternately, forming a zeolite-like framework. The lattice is riddled with micro- and mesopores, endowing ZIF-8 with an expansive surface area, robust thermal/chemical resilience, and superior adsorption capacity. Additionally, ZIF-8 is sensitive to changes in solution pH; its structure is easily decomposed under acidic conditions and is relatively stable under neutral conditions, enabling controlled release of loaded drugs. ZIF-8 also exhibits favorable biocompatibility and biodegradability. Thanks to these attributes, it serves as a promising nanocarrier: Meng et al. [32] impregnated the framework with curcumin, achieving a drug load of 11.6 % and an encapsulation efficiency of ~83 %. Furthermore, ZIF@CCM showed pH-responsive drug release behavior and chemo-photodynamic therapy, exhibiting excellent antibacterial activity.

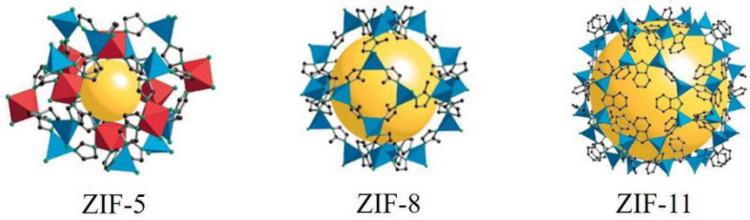

Figure 2 Structural diagrams of three common ZIFs[33]

2.2.2 MIL Series (Materials of the Lavoisier Institute)

The MIL family (Fig. 3) was unveiled by Férey's team at the Université de Versailles–Saint-Quentin. Its members fall into two broad classes: frameworks built from lanthanide or transition-metal nodes cross-linked by simple di-carboxylates such as glutarate or succinate [34]. The other is composed of trivalent metals such as Cr^{3+}, Fe^{3+},

Al^{3+}, etc., coordinated with carboxylic acid ligands like terephthalic acid or trimesic acid. The characteristic of this type of material is the "breathing phenomenon," where the material can change between narrow and wide pore sizes under the stimulation of external conditions [35]. Among the MILs series materials, the most representative are MIL-101, MIL-53, and MIL-100, which have good stability. Han et al. [36] showed that decorating MIL-101(Cr) with amino groups—yielding MIL-101(Cr)-NH_2—boosts CO_2 capture to 5.4 mmol g^{-1} at 1 bar/278 K and, under a 0.15 bar CO_2 / 0.85 bar N_2 flue-gas mix, outperforms the parent framework in CO_2/N_2 selectivity.

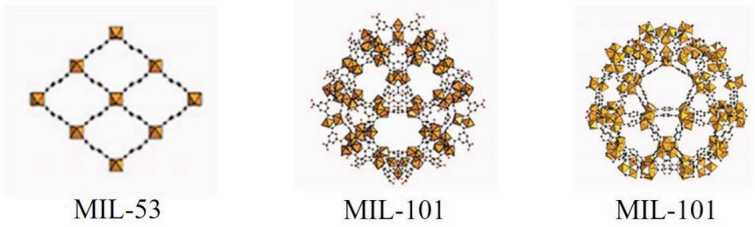

Figure 3 Structure diagram of three types of MILs[37]

2.2.3 Zr-MOF Series (Zirconium-based Metal-Organic Frameworks)

In 2008, the Lillerud research group at the University of Oslo in Norway prepared three types of MOF materials formed by zirconium-containing ions and dicarboxylic acid organic ligands, with octahedral cage-like and eight tetrahedral corner cage-like structures, named UiO-66, UiO-67, and UiO-68 [38, 39]. Among them, the UiO-66 material (as shown in Fig. 4) has received the most attention. It is synthesized from the inorganic metal unit $[Zr_6O_4(OH)_4]$ and 1,4-benzenedicarboxylic acid. Due to its large coordination number and the very strong Zr-O interaction force, UiO-66 has good thermal and chemical stability, maintaining its structure stable in high temperatures and strong acid or alkali solutions [40, 41]. Gao et al. [42] grew 20–200 nm UiO-66-NH_2 nanocrystals, loaded them with 5-FU, and surface-functionalized the particles with folic acid for tumor targeting and 5-FAM for fluorescence tracking. The resulting UiO-66-NH_2-FA-5-FAM/5-FU conjugate enabled targeted delivery, real-time imaging, and potent tumor growth inhibition. Subsequently, MOFs based on metal zirconium were gradually developed. A large number of researchers have used high-coordination-number metals such as Zr^{4+} and Hf^{4+} as metal cluster cores, coordinated with carboxylic acid ligands of different lengths and types, to prepare various MOF materials with good stability, such as MOF-525, MOF-545, MOF-808, DUT-67, DUT-69, DUT-80, and BUT-39.

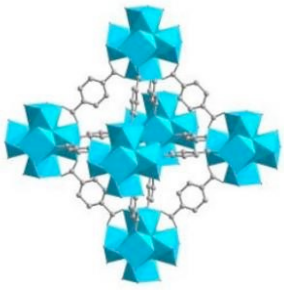

Figure 4 Structure diagram of UiO-66[43]

2.2.4 IRMOF Series (Isoreticular Metal-Organic Frameworks)

The IRMOF series materials (as shown in Fig. 5) were first discovered by the Yaghi group at the University of California, Berkeley, and named "IRMOFs". These MOFs crystallize as octahedra in which $[Zn_4O]^{6+}$ clusters act as six-connected nodes that are stitched together by various aromatic carboxylate linkers. The representative material of this series is IRMOF-1, also known as MOF-5 [44]. By replacing the organic ligand of IRMOF-1, a series

of IRMOFs with the same structure but different pore sizes can be obtained [45]. In 2002 Yaghi's group [46] systematically lengthened the aromatic dicarboxylate struts to engineer IRMOFs whose apertures span 0.38–2.88 nm, a demonstration that rapidly drew wider interest. Cai et al. [47] later impregnated curcumin into IRMOF-1 and IRMOF-3; the amino-decorated variant achieved a 55 % drug load—outpacing the 49 % recorded for the parent framework—and released the cargo more gradually, underscoring its superior sustained-release profile. Both carriers proved minimally cytotoxic and biologically benign.

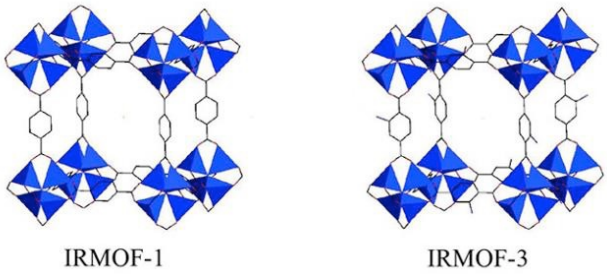

Figure 5 Structural diagrams of IRMOF-1 and IRMOF-3 [47]

2.2.5 PCN Series (Porous Coordination Networks)

PCN series materials are topological structure materials with pore-cage and pore-channel structures formed by copper and organic ligands such as trimesic acid [48]. The flagship member of this lineage is HKUST-1—also tagged Cu-BTC or MOF-199—first assembled in 1999 by Williams' team at the Hong Kong University of Science and Technology (Fig. 6). This type of material is widely used in gas storage and heterogeneous catalysis. For example, Lin et al. [50] prepared HKUST-1 and studied its hydrogen storage capacity. HKUST-1 crystals (15–20 μm) gave a classic Type-I N_2 isotherm and a BET area of 1055 $m^2\ g^{-1}$; H_2 uptake reached 0.47 wt % at 303 K under 35 bar.

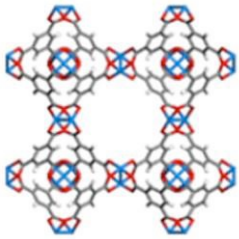

Figure 6 Structure diagram of HKUST-1 [51]

2.2.6 CPL Series (Coordination Pillared-Layer Materials)

CPL frameworks (Fig. 7) are built by linking six-coordinate metal centers with neutral N-heterocyclic pillars—2,2′-bipyridine, 4,4′-bipyridine or phenanthroline—to yield porous coordination polymers, of which CPL-1 is the archetype [52].Chen et al. [53] reported that CPL-1 can highly selectively separate C_3H_6/C_3H_8 at 273 K and is easily regenerated at 298 K.

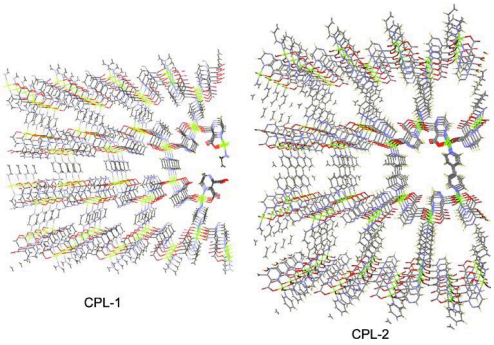

Figure 7 Structure diagram of CPL-1 and CPL2[52]

2.2.7 ZJU Series

The ZJU family—designated and developed at Zhejiang University—includes frameworks such as ZJU-137, luminescent ZJU-168-Eu (Fig. 8) and ZJU-74a. This series of materials is widely used in sensing, gas separation, and storage [54, 55]. For example, Pei et al. [56] reported a chemically stable Hoffmann-type metal-organic framework named ZJU-74a for the selective capture of C_2H_2. Gas adsorption isotherms showed that ZJU-74a has the highest C_2H_2 capture capacity to date (49 cm^3/g at 0.01 bar and 296 K).

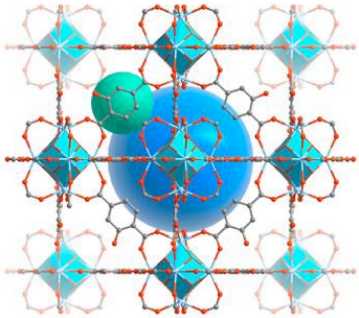

Figure 8 Structure diagram of ZJU-168 (Eu) [57]

2.3 Applications of MOFs

MOFs have been extensively researched due to their high porosity, ease of functionalization, large specific surface area, and excellent biocompatibility, showing great application prospects in adsorption, catalysis, imaging, drug carriers, and analytical detection.

2.3.1 Adsorption

Thanks to their vast surface areas and open porosity, MOFs serve as high-capacity sorbents for organic contaminants, trace metals and gases—including CO_2, CO and H_2S. Singh et al. [58] successfully synthesized a novel dual-responsive CaFu MOF that can simultaneously adsorb and remove imidacloprid (a highly consumed pesticide) and highly toxic Cd(II) (as shown in Fig. 9). Under the same conditions, CaFu MOF trapped 467 mg g^{-1} of imidacloprid and 781 mg g^{-1} of Cd^{2+}. Dilute hydrochloric acid could desorb the adsorbed pollutants from the adsorbent, and the material could be reused for 5 adsorption-desorption cycles without significant loss of adsorption capacity. Yurduses et al. [59] enhanced the CO_2 adsorption capacity of MIL-88B by adjusting the Fe/BDC ratio and synthesis temperature to control the hierarchical pores. The results showed that the maximum CO_2 adsorption capacity of MIL-88B was 5.58 wt% (at 1 bar and 298 K), which was greater than the reported CO_2 absorption capacities of commercial MOFs (MOF-5: 4.5 wt%; ZIF-8: 4.3 wt%).

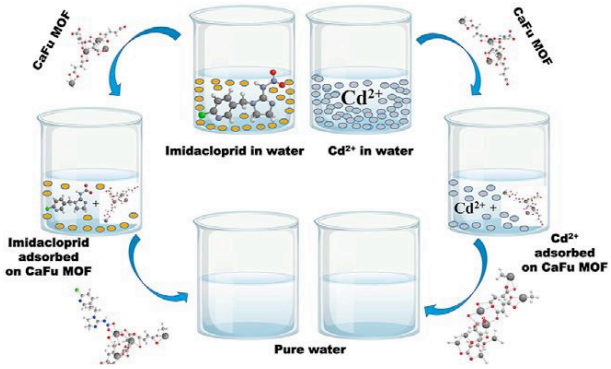

Figure 9 Schematic diagram of CaFu MOFs for removing imidacloprid and Cd (II) from water [58]

2.3.2 Catalysis

MOFs offer densely populated active sites, high porosity and engineerable apertures, ensuring rapid substrate access and facile diffusion of both reactants and products [60]. Therefore, MOFs are widely used in photocatalysis and electrocatalysis. Gong et al. [61] unveiled Ce-TTCA, a robust Ce-MOF that, after Pt decoration, evolves H_2 at 60 μmol g^{-1} h^{-1} in pH 2 medium and 349 μmol g^{-1} h^{-1} in pH 12 medium. Partial Ce^{3+} → Ce^{4+} oxidation widens light harvesting and accelerates charge separation; a 64 % Ce^{4+} sample (Pt/Ce-TTCA-65) outperforms the fully Ce^{3+} analogue by six-fold. Nie et al. [62] meanwhile embedded Pd nanoparticles inside a high-porosity MOF (Fig. 10); the resulting Pd/MOF delivers a Tafel slope of 85 mV dec^{-1} and requires only 105 mV overpotential for acidic HER, thanks to the synergistic interplay between Pd sites and the MOF scaffold.

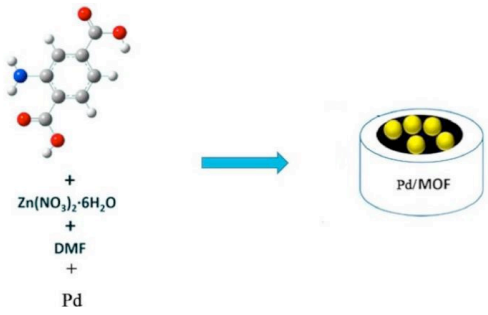

Figure 10 Schematic diagram of MOF synthesis [62]

2.3.3 Imaging

Theranostics—an evolving paradigm that fuses real-time imaging with on-demand therapy—relies on carriers that are simultaneously drug depots and contrast agents [63]. Thanks to their ultra-large surface areas and open porosity, MOFs are emerging as prime scaffolds for such dual-purpose platforms. Gao et al. [42] synthesized UiO-66-NH_2 with particle sizes in the range of 20-200 nm, which can be used to transport the antitumor drug 5-FU. Simultaneously, they covalently grafted the targeting agent folic acid (FA) and the fluorescent imaging agent 5-hydroxyfluorescein (5-FAM) to construct a UiO-66-NH_2-FA-5-FAM/5-FU targeted drug delivery and imaging system. Qin et al. [64] engineered Mn-doped Ti-MOF nanosheets (Mn-Ti MOFs) that behave as dual-mode microwave sensitizers (Fig. 11). Their porous lattice converts microwave energy into heat via ion-confinement collisions (MWTT), while Mn-induced defects narrow the band-gap and boost e^-/h^+ separation, permitting robust ROS generation at only 2 W (MWDT). The same Mn centers simultaneously provide T_1-weighted MRI contrast, enabling real-time visualization of intratumoral accumulation and on-the-spot guidance of microwave exposure. PEGylated Mn-Ti MOFs eradicated hepatic tumors in vitro and in vivo under low-power irradiation, underscoring their potential as MRI-guided theranostic platforms and expanding the biomedical repertoire of Ti-based MOFs.

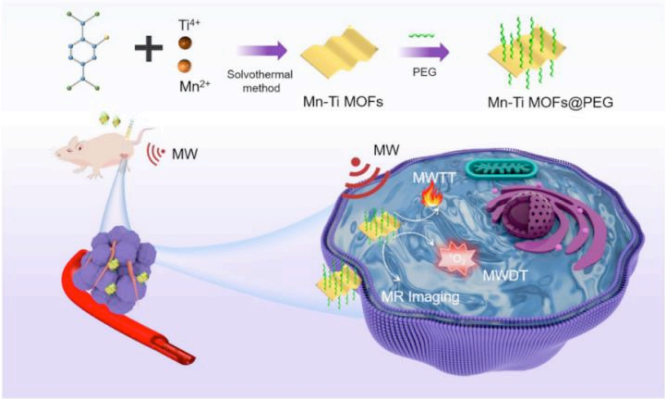

Figure 11 Mn Ti used for magnetic resonance imaging and microwave dynamic hyperthermia (MWDT-MWTT) MOFs@PEG Schematic diagram of the synthesis process of nanosheets[64]

2.3.4 Drug Carriers

Engineering delivery platforms that release drugs on demand is essential for minimizing off-target toxicity and maximizing therapeutic benefit [65]. MOFs have unique advantages in drug delivery systems due to their tunable shape, size, pore size, and functionality, high loading capacity, degradability, high stability, and low cytotoxicity. Mi et al. [66] built a tumor-seeking nanovehicle by growing ZIF-8 around baicalein (BAN) and capping the surface with folate-PEG (PEG-FA@ZIF-8@BAN, Fig. 12). The resulting dispersion (176 nm, −24 mV) entrapped 41 % drug and remained closed at pH 7.4 (<11 % leakage), yet liberated its payload rapidly at pH 5.0. FA-directed uptake amplified BAN cytotoxicity in FR-positive MCF-7 cells, and orthotopic breast-cancer mice treated with the formulation showed markedly enhanced tumor growth suppression compared with free drug or non-targeted controls..

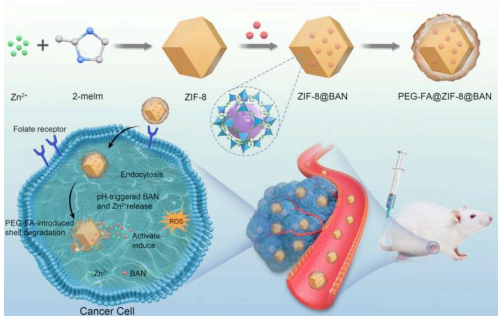

Figure 12 PEG-FA@ZIF-8 @Schematic diagram of BAN nanoplatform formation and effective anti-tumor therapy of folate receptor-mediated responsive drug delivery system [66]

2.3.5 Analysis and Testing

Due to the dual characteristics of inorganic and organic absence in MOFs skeletons, they have great prospects in the field of analyzing and detecting environmental pollutants and biomarkers in biological fluids. Song et al. [68] introduced NPCN-222-ATP, a nanosized, porphyrin-ATP-based chiral MOF that reports alkaline-phosphatase (ALP) activity through simultaneous fluorescence and color read-outs (Fig. 13). The probe distinguishes ALP down to 0.024 mU mL^{-1} (fluorescence) and 0.023 mU mL^{-1} (color), outperforming current assays, and permits real-time ALP imaging in live cells, validating enantio-pure MOFs as analytical platforms. Wang et al. [69] designed Eu-MOF BUC-88 that differentiates quinolones from tetracyclines by both emission intensity and visible hue. It detects enrofloxacin, norfloxacin and ciprofloxacin with limits of 0.12, 0.52 and 0.75 µM, respectively, and responds to tetracycline hydrochloride within one second at 0.08 µM. Spiked-lake-water recoveries for the four antibiotics ranged from 99.8 % to 102.3 %, demonstrating naked-eye ultrasensitive screening.

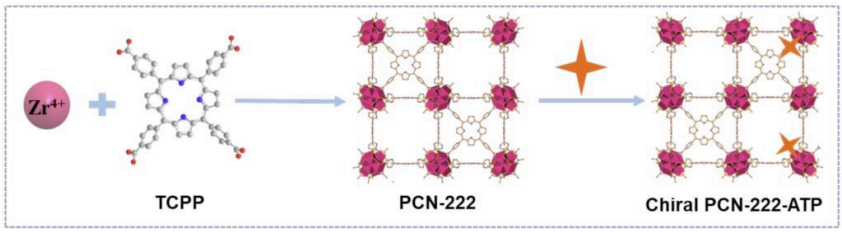

Figure 13 Schematic diagram of the synthesis of nanoscale chiral MOFs (NPCN-222-ATP) probe based on porphyrin adenosine triphosphate [68]

3. Nanoscale Drug Carriers

3.1 Introduction to Nanoscale Drug Carriers

Nanoscale drug carriers are tiny drug carrier delivery systems, typically with particle sizes below 500 nm. As drug-delivery vehicles, nanomaterials are typically solid colloidal particles 10–1000 nm in size and built from natural or synthetic polymeric scaffolds. They form drug control systems by chemically bonding, physically adsorbing, or encapsulating drug molecules in various forms. With the rapid development of porous materials, nanoporous materials as drug carriers have also attracted widespread attention from researchers. Encapsulating drugs in microparticles can regulate drug release rates, increase permeability across biological membranes, alter in vivo distribution, and improve bioavailability. Below is a brief introduction to common nanoscale drug carriers.

3.2 Common Nanoscale Drug Carriers

3.2.1 Liposomes

Liposomes are completely enclosed miniature multilamellar vesicles formed by phospholipids and other lipoids into bilayers. They can encapsulate drugs within the lipid bilayer and transport them to the lesion site. Liposomes were first discovered by Bangham et al. [70] in 1965. It wasn't until the 1990s that Gregoriadis et al. [71] used drug-encapsulated liposomes as a drug delivery system. Liposomes have attracted more attention due to their low toxicity, degradability, and good biocompatibility [72, 73]. Li et al. [74] designed an aromatized liposome to improve sustained drug release. Data revealed that aromatized liposomes boosted drug payload while markedly slowing the release of compounds spanning a wide range of water solubilities and molecular weights. Aromatized liposomes extended the duration of local anesthesia with TTX (tetrodotoxin, a local anesthetic) to over 3 days and reduced systemic toxicity. Yang et al. [75] embedded nanobowls into liposomes (NbLipo) to enhance the stability of the drug DOX (as shown in Fig. 14). DOX@NbLipo exhibited high doxorubicin loading and withstood leakage triggered by plasma proteins and hemodynamic shear, boosting tumor accumulation and therapeutic efficacy.

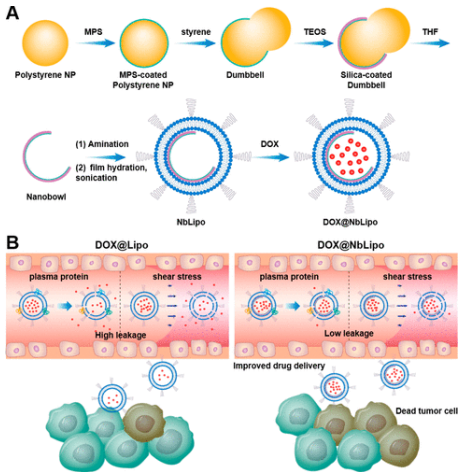

Figure 14 (A) DOX@NbLipo Schematic diagram of the formulation, (B) The role of the nanobowl in preventing DOX leakage caused by plasma protein and blood flow shear stress, which can lead to more drug delivery to the tumor site [75]

3.2.2 Polymeric Nanoparticles

Polymeric nanoparticles are typical "soft" carriers, built from a polymer core encased in an outer shell. Their surface can be modified with different chemical structures to achieve various functional changes [76]. Polymeric nanoparticles—valued for their biocompatibility, degradability and high surface area—continue to expand their biomedical footprint. Huang et al. [77] produced PLGA cores that co-entrap the Aβ-modulating peptide S1 and curcumin, then cloaked the surface with brain-homing CRT peptide to enhance BBB crossing (Fig. 15). In APP/PS1 mice the nanosystem restored spatial memory and recognition, lowered cerebral Aβ, ROS, TNF-α and IL-6, elevated SOD activity and increased synaptic density. Lu et al. [78] similarly fabricated paclitaxel-loaded PLGA spheres whose cationic chitosan corona raised encapsulation to 87 %, suppressed the initial burst, and conferred pH-sensitive release (66.9 % to 14.3 % after 2 h depending on CS density). The particles released PTX faster at pH 5.5 than at 7.4 and showed superior uptake and cytotoxicity in MDA-MB-231 cells relative to plain PLGA or free drug.

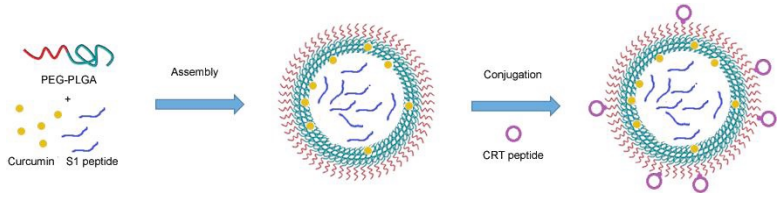

Figure 15 Schematic diagram of PLGA nanoparticle manufacturing [77]

3.2.3 Gold Nanoparticles

Gold nanoparticles are a novel type of inorganic nanoscale drug-carrying particle. Thanks to superior biocompatibility, straightforward synthesis, facile surface engineering and efficient targeting, gold-based nanosystems are increasingly exploited for diverse therapies [79,80]. Sivaji et al. [81] coated ~80 nm AuNPs with polysorbate 80-PEG and loaded them with donepezil (GNPD) to ferry the anti-Alzheimer agent across the BBB. In zebrafish GNPD boosted brain AChE inhibition by 30–38 % and doubled Au retention on day 1 (still +22 % at day 15), while histology revealed no pia-mater aggregation seen with bare AuNPs. Zhang et al. [82] instead grew Au nanorods inside mesoporous MnO_2 shells, adsorbing DOX via electrostatics, H-bonding and physical entrapment (Fig. 16). The hybrid achieved 99 % drug loading, released 47 % within 12 h, and disintegrated in response to high GSH, acidic pH or NIR irradiation, affording triple-triggered on-demand therapy.

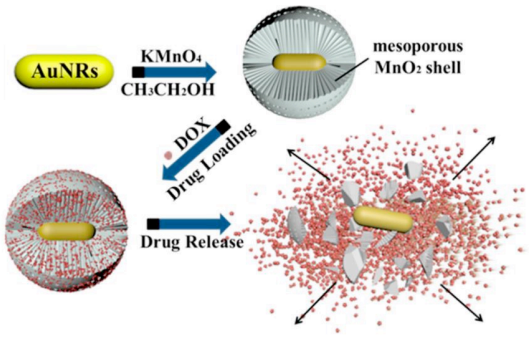

Figure 16 Schematic diagram of preparation and drug release of Au/MnO2 nanoparticles [82]

3.2.4 Mesoporous Silica

Owing to its natural abundance, proven biocompatibility, vast surface area and straightforward silanation chemistry, mesoporous silica was the first inorganic scaffold adopted for drug delivery and remains a mainstay of the field [83]. Niemelä et al. [84] anchored the folate antagonist methotrexate onto MSN surfaces to create FR-targeted vehicles that were subsequently loaded with the immunomodulator fingolimod (FTY720) (Fig. 17). The construct curbed proliferation and invasion of anaplastic thyroid cancer cells while sparing normal thyroid epithelia; in mice it suppressed xenograft infiltration and shifted tumor pathology toward necrosis, outperforming free-drug cocktails. Ying et al. [85] likewise tethered 5-aminosalicylic acid (5-ASA) to silica colloids (5-ASA-SiO_2) for ulcerative-colitis therapy. The composite displayed cytotoxicity on par with free 5-ASA and neat SiO_2, yet a low dose of the nanoparticle formulation matched the therapeutic benefit of a high dose of free drug, as evidenced by marked reductions in disease activity index and colonic histopathology scores.

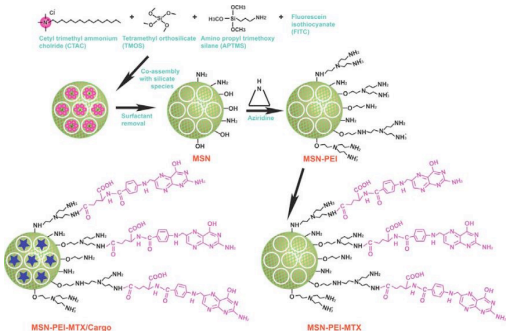

Figure 17 Schematic diagram of synthesis and functionalization of MSNs designed [84]

3.2.5 Carbon Nanomaterials

Carbon nanomaterials (CNMs) are grouped by dimensionality: 0-D fullerenes, 1-D carbon nanotubes (CNTs), and 2-D graphene. Their standout thermal/electrical conductivities, mechanical robustness and tunable optics have propelled them into the biomedical spotlight [86]. Lohan et al. [87] developed multi-walled carbon nanotubes (MWCNTs) loaded with berberine (BRB) for treating AD, coated with phospholipids and polysorbate. The optimized multi-walled carbon nanotubes (MWCNTs) displayed a mean diameter of 186 nm, entrapped 68.6 % of the payload and liberated 96 % within 16 h. After surfacing with polysorbate plus phospholipids, the tubes reversed memory deficits in an AD model between days 18–20 and restored normal brain biochemistry, underscoring their anti-amyloid potential. Gooneh-Farahani et al. [88] used MD simulations to compare doxorubicin (DOX) and paclitaxel (PAX) loading on pH-responsive fullerenes (Fig. 18). Carboxylated C_{60} bound DOX tightly via electrostatics, enabling tumor-selective release, whereas neutral PAX required decoration with trimethyl-chitosan (TMC). The polymer boosted van-der-Waals contacts and H-bonding at pH 7.4; once acidity drove TMC protonation, these forces collapsed to zero, triggering PAX discharge in the cancer milieu.

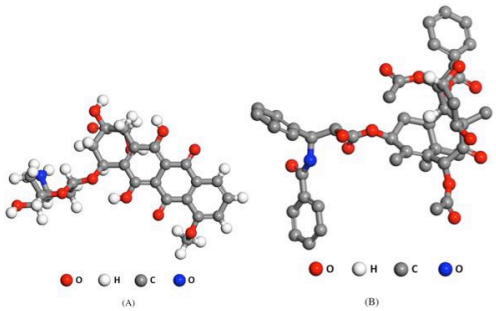

Figure 18 Molecular structure of DOX, (B) Molecular structure of PAX [88]

3.2.6 Metal-Organic Frameworks (MOFs)

MOFs are an emerging class of nanomaterials that have become a research hotspot in recent years as drug carriers due to their unique advantages. Singh et al. [89] synthesized a pH-responsive folic acid (FA) and graphene oxide (GO) modified ZIF-8 (GO-FA/ZIF-8) for the simultaneous targeted delivery of doxorubicin (DOX) and cyclophosphamide (CP). Through the cleavage of chemical bonds and the destruction of the MOF structure under acidic conditions (pH 5.6), the DOX@ZIF-8/GO-FA/CP nanocarrier showed pH-responsive sustained release characteristics in vitro (76% of DOX and 80% of CP). Against MCF-7 and MDA-MB-231 cells, DOX@ZIF-8/GO-FA/CP produced clear synergy (CI = 0.29 and 0.75, respectively) versus the free-drug cocktail, validating the platform as an intelligent, ratio-controlled co-delivery vehicle for breast-cancer therapy. Yu et al. [90] meanwhile fused ceria nanozymes with MIL-100 to create CeNPs/RA@MIL-100/siSOX9 (CeRMS). The MOF shuttles siSOX9 and retinoic acid while the embedded ceria scavenge ROS, synchronously enhancing neurogenesis and directional neuronal differentiation. In aged 3xTg-AD mice, CeRMS elevated newborn neuron counts and reversed memory deficits, offering a nanozyme-powered strategy for neuroregeneration.

3.2.7 Covalent Organic Frameworks (COFs)

Covalent organic frameworks (COFs) are 2-D or 3-D crystalline polymers whose light-element backbones—C, H, N, O, B, S—are stitched into predictable, permanently porous lattices through robust covalent linkages. Due to their good thermal and chemical stability, tunable pore size, highly ordered pore channel structure, and modifiability, they have become emerging candidate materials in the biomedical field. Liu et al. [91] encapsulated DOX in a single-step COF synthesis, attaining 32 wt % loading. The construct remained largely closed at pH 7.4 (~40 % release in 2 h), yet discharged its cargo within the same period at pH 5.0–6.5, finishing delivery after 24 h. Furthermore, after injection of DOX@COF, the tumor volume in mice significantly decreased, indicating that DOX@COF had good antitumor efficacy. Pathological analysis of the main organs (heart, liver, spleen, lungs, and kidneys) of the mice showed no significant pathological damage or changes in these organs, indicating that DOX@COF had good biocompatibility in vivo. Jia et al. [92] grew an 8-hydroxyquinoline-tagged COF-HQ that hosted 73 μg 5-FU mg^{-1}. Over 48 h the composite released 48 % at pH 7.4 versus 62 % at pH 5.0, confirming sustained, acidity-accelerated delivery. Even at 250 μg mL^{-1} the blank COF-HQ left 93 % of cells viable, while 5-FU@COF-HQ retained potent tumor growth inhibition, underscoring both safety and therapeutic utility..

4. Preparation and Application of Nanoscale CD-MOFs

4.1 Preparation of Nanoscale CD-MOFs

CD-MOFs have superior biocompatibility. CD-MOFs are composed of γ-cyclodextrin and potassium ions. The essence of γ-CD is a symmetric cyclic oligosaccharide formed by D-glucopyranose connected through α-1,4-glycosidic bonds. Produced by enzymatic hydrolysis of natural starch, γ-cyclodextrin (γ-CD) is essentially non-toxic (LD_{50} > 5 g kg^{-1}) and readily encapsulates hydrophobic guests to boost their water solubility—an asset already exploited in food, cosmetic and biomedical formulations. Combining this renewable macrocycle with physiological potassium gives CD-MOF: colourless body-centred cubes crystallize within a week when methanol vapour slowly diffuses into an 8:1 KOH/γ-CD aqueous solution at room temperature, affording a 54 % porous, bio-friendly framework under remarkably mild conditions. The $(CD)_6$ structural unit forming CD-MOF has a central hydrophilic spherical pore channel of 1.7 nm. The inner surfaces of two adjacent γ-CD molecules form a hydrophobic pore channel of 1.0 nm. There are also triangular pores of 0.4 nm along the [111] axis plane of the crystal. These pores of different sizes are arranged regularly, collectively forming the rich pore structure of CD-MOF, providing ample space for drug loading. Furthermore, CD-MOF has both hydrophilic and hydrophobic pore channels, allowing it to load both hydrophobic and hydrophilic drugs. Therefore, CD-MOF has broad application prospects in drug delivery.

CD-MOF has good safety, but as a qualified drug carrier, it should also have a suitable particle size. Usually, CD-MOF crystals prepared by the slow volatilization method have a particle size of about 40-500 nm. CD-MOF crystals of this size cannot enter capillaries and the lymphatic circulation, making them unable to be effectively taken up by cells and difficult to apply in the biomedical field. Translating CD-MOF into drug-delivery applications hinges on generating monodisperse nanoscale crystals [6]; downsizing the framework without sacrificing porosity or crystallinity has therefore become a central focus of current research. Studies have shown that

adding an appropriate amount of the surfactant cetyltrimethylammonium bromide (CTAB) during the preparation of CD-MOF by the solvent diffusion method can slow down crystal growth speed, increase the number of nuclei, and obtain CD-MOF with a size of 200-300 nm. Liu et al. further improved the solvent diffusion method. They found that pre-adding 10% (v/v) methanol to the KOH solution of γ-CD, then incubating the crystals at 50°C for 6 hours, and finally adding CTAB to adjust the MOF morphology, could yield uniformly sized micron and nano CD-MOF. This optimized solvent diffusion method shortened the preparation time of CD-MOF from 1 week to 6 hours without changing the crystallinity and porosity of the crystals. They showed that crystal size can be dialed in by tuning reactant concentration, temperature, aging time, the γ-CD/KOH ratio, and the level of surfactant employed. Liu et al. also found that microwave-assisted synthesis could quickly obtain CD-MOF with a size of 100-300 nm. Additionally, Qiu et al. reported a method for preparing nanoscale CD-MOF using short-chain amylose nanoparticles as seeds combined with the anti-solvent method [.OI]. Among these methods, the improved solvent diffusion method is the preferred method for laboratory preparation and research of CD-MOF due to its simple operation, mild conditions, low instrument requirements, controllable particle size, and high yield.

4.2 Applications of CD-MOF in Drug Delivery

Current data show that CD-MOF couples classical MOF assets—well-defined lattice, ultra-high surface area and open porosity—with intrinsically low toxicity, green aqueous synthesis, low cost and facile scale-up, positioning it as a highly attractive platform for biomedical applications. Currently, there have been reports of successful loading of drug molecules into CD-MOF. CD-MOF loads drugs through weak interactions between the drug and the carrier, specifically physical adsorption or co-crystallization. Studies have shown that using CD-MOF to encapsulate guest molecules not only results in high encapsulation efficiency but also effectively improves the physical and chemical stability of the guest molecules and significantly increases their solubility and bioavailability. Moussa et al. found that compared to free curcumin, the phenolic hydroxyl groups of curcumin inside CD-MOF form hydrogen bond interactions with the hydroxyl groups on cyclodextrin, increasing its storage stability by at least three orders of magnitude. Moreover, when curcumin-loaded CD-MOF is dispersed in water, the CD-MOF gradually disintegrates. However, curcumin does not directly detach from the CD-MOF framework; instead, it forms a special adduct with free γ-CD and K^+ through complexation, further avoiding the chemical degradation of curcumin. Zhang et al. found that after loading vitamin A palmitate (VAP) into CD-MOF, the chemical instability caused by the conjugated double bonds and ester bonds in the VAP structure could be effectively inhibited. Studies found that the encapsulation efficiency of VAP could be as high as (9.77 ± 0.24)%. No extra antioxidant was needed: VAP stability rose sharply and its half-life lengthened 1.6-fold. Likewise, Inoue et al. showed that entrapping coenzyme Q_{10} inside CD-MOF creates a crystalline solid dispersion (CoQ/CD-MOF-1) in which CH···OH hydrogen bonds between the isoprenoid side-chain and the framework boost solubility ~100-fold and markedly elevate oral bioavailability. The co-crystal formed by the non-steroidal anti-inflammatory drug ibuprofen and CD-MOF could achieve a drug loading capacity of 26% (wt). Although the co-crystal had similar blood uptake speed and bioavailability to pure potassium ibuprofen salt, the half-life of ibuprofen was doubled, not only quickly relieving pain but also prolonging the analgesic time. Xu et al. found that nanoclusters of the poorly soluble drug folic acid (FA) could simultaneously occupy two pore sizes in CD-MOF, 0.78 and 1.7 nm, obtaining FA/CD-MOF with high drug loading capacity. Compared to free folic acid, FA/CD-MOF not only increased the stability of FA but also increased the apparent solubility of folic acid by 1450 times and the bioavailability AUC by 1.48 times. He et al. found that azilsartan (AZL) could also exist in the form of nanoclusters inside CD-MOF. Compared to the pure drug, the apparent solubility of AZL/CD-MOF was increased by 340 times, and the bioavailability in rats was 9.7 times that of AZL. CD-MOF has also been exploited to host a broad spectrum of guests—anti-inflammatory agents (diclofenac, flurbiprofen, fenbufen, ketoprofen, piroxicam), ACE inhibitors (captopril), proton-pump inhibitors (lansoprazole), nutraceuticals (curcumin, sucralose), dyes (4-phenylazophenol, rhodamine B) and other actives (salicylic acid, ferulic acid)—stabilizing the compounds, raising their apparent solubility and affording sustained release.

4.2.1 Drug Delivery Systems Based on AD

AD is currently one of the most difficult diseases to cure, and the presence of the BBB further increases the difficulty of treatment. Therefore, various drug delivery systems for AD have been developed. Yang et al. [93] encapsulated rivastigmine in CPP-decorated liposomes (CPP-Lp, Fig. 1-21) to boost brain uptake and curb oral

side-effects. At pH 5.0 the nano-vehicle prolonged in-vitro release versus free drug, and BBB-Papp values after 24 h rose progressively from 3.36×10^{-6} cm s^{-1} (solution) to 3.77×10^{-6} cm s^{-1} (plain Lp) and 3.96×10^{-6} cm s^{-1} (CPP-Lp), confirming enhanced transport. CPP-Lp improved the ability to penetrate the BBB. After administration for a certain time, CPP-Lp could quickly distribute throughout the systemic circulation. Pharmacodynamic results showed that after administration, the activities of acetylcholinesterase and cholinesterase in rats decreased, indicating that CPP-Lp could inhibit the activities of these two enzymes, helping to reduce cholinergic defects. Joshi et al. [94] used polymer PLGA and PBCA nanoparticles as carriers to prepare a sustained-release nanoparticle formulation loaded with rivastigmine tartrate (RT). In vitro studies showed that PLGA and PBCA nanoparticles released 30.86 ± 2.07% and 43.59 ± 3.80% of RT within 72 hours, respectively. Pharmacokinetic studies showed that compared to the RT solution, amnesia mice using PLGA and PBC nanoparticles recovered memory faster, meaning RT could be transported to the mouse brain faster and to a greater extent. Therefore, both nanoparticles are suitable as potential carriers for providing sustained brain delivery of RT. Yang et al. [95] crafted single-walled carbon nanotubes loaded with acetylcholine (SWCNT-ACh). After treatment, AD mice regained normal learning ability in a dose-dependent manner; doses ≤ 300 mg kg^{-1} avoided toxicity, highlighting SWCNTs as viable neural carriers. Kim et al. [96] synthesized anemonin-PEG-gold nanoparticles (An-PEG-AuNPs). The particles were non-toxic to HT22 cells (85–95 % viability), crossed the BBB, and in $A\beta_{1-42}$ mice reduced Aβ and BACE-1 levels, blocked tau hyper-phosphorylation via GSK-3β/CDK5, suppressed microglial/astrocytic activation and alleviated neuro-inflammation and degeneration. Santos et al. [97] entrapped the anti-amyloid natural product magnolol inside UiO-66(Zr), creating Mag@UiO-66(Zr) particles that combine neuroprotection with MOF-controlled release. β-secretase inhibition activity research results showed that Mag@UiO-66(Zr) had a good inhibitory effect on β-secretase. Furthermore, Mag had a strong binding affinity for possible targets of AD. Finally, Mag@UiO-66(Zr) prevented further neuronal damage or reversed neuronal damage. In summary, the Mag@UiO-66(Zr) designed in this study had better neuroprotective effects and therapeutic efficacy.

4.2.2 Drug Delivery Systems Based on Cancer

Cancer incidence is on the rise globally and has emerged as a major threat to human health and life expectancy. However, due to the existence of biological barriers, the therapeutic effect has not met expectations. The establishment of drug delivery systems has alleviated this problem to some extent. Li et al. [98] synthesized silica nanoparticles with a thyrotropin receptor-targeting ligand (TSH-SiO_2@Dox). This ligand can specifically target thyroid cancer, and the encapsulated Dox can be acid-triggered to release the drug for cancer treatment (as shown in Fig. 1-22). The drug loading capacity of this nanoparticle was 3 w/w%, and the encapsulation efficiency was 45.4%. In a buffer at pH 7.4, 40% of Dox was released within 72 hours, while it was almost completely released in a buffer at pH 5.0. Flow cytometry results showed that TSH-SiO_2@Dox had a targeting effect. In vivo antitumor results showed that tumor growth in mice was almost inhibited after treatment with TSH-SiO_2@Dox. Asad et al. [99] prepared chitosan nanoparticles loaded with carboplatin (CP) (CPLCs NPs) for treating breast cancer. The maximum encapsulation efficiency and loading rate of carboplatin were 58.43% and 13.27%, respectively. In vitro release profiles of carboplatin displayed a biphasic pattern: an initial burst releasing 32.66 % at pH 5.0 and 23.53 % at pH 7.4 within 20 h, followed by sustained delivery over the next 120 h. Cytotoxicity study results of CPLCs NPs showed that CPLCs NPs had good antiproliferative effects, also showed greater cellular uptake, and chitosan nanoparticles were non-toxic within a certain concentration range and time. Lila et al. [100] oxidized graphene nanoribbons, tagged them with folic acid (OGNRs-FA) and loaded tamoxifen citrate (TC). The multi-layer construct entrapped 56 % of the drug and released >90 % at pH 7.4 but only 68 % at pH 4 within 72 h. MTT assays on MCF-7 and MDA-MB-231 cells revealed concentration- and time-dependent killing that exceeded free TC, while FA coating markedly increased intracellular accumulation; in-vivo studies confirmed slower systemic leakage and higher tumor exposure. Amreddy et al. [101] assembled folate-decorated PAMAM dendrimers (Den-PEI-CDDP-siRNA-FA) that co-delivered cisplatin and HuR siRNA to FR-α-high H1299 lung cancer cells. Folate conjugation left both CDDP (≈28 %) and siRNA (≈34 %) release kinetics unchanged, yet boosted uptake and endosomal escape. Targeted particles silenced HuR mRNA, down-regulated cyclin E and produced 62 % growth inhibition—superior to non-targeted controls. Gupta et al. [102] solvothermally grew UiO-66, loaded docetaxel (DTX@UiO-66) and over-coated with PEG. The shell retarded diffusion, stretching release to 96 h at pH 7.4 (64 %) versus 60 h (92 %) for uncoated particles at pH 5. PEG@DTX@UiO-66 retained dose-dependent cytotoxicity, time-dependent uptake and pro-apoptotic activity while the bare MOF showed minimal toxicity, confirming carrier safety.

4.2.3 MOF-Based Drug Loading and Therapy for Cancer

By cloaking drugs inside nanocarriers, nano-delivery systems create a physical shield that keeps enzymes, bile salts and other aggressive blood components from attacking the payload, markedly prolonging drug integrity in circulation [102].

Nano-drug delivery systems can improve the bioavailability of drugs. After oral administration, some macromolecular drugs are easily affected by relevant enzymes in intestinal epithelial cells, making it difficult to exert their true effects. Nano-drug delivery systems can well improve this shortcoming, increase the permeability of drugs on biomembranes, enable them to better pass through barriers and enrich in tumor tissues, improve the bioavailability of drugs, and increase utilization rates [103].

Nano-drug delivery systems have targeting capabilities. Firstly, due to the rapid proliferation of tumor cells, the vascular walls formed around them are incomplete, resulting in the formation of a large number of nano-sized pore-like gaps. Nano-drug delivery systems can pass through these gaps and truly reach the diseased tissue or organ. Secondly, when designing and preparing nano-drug carrier particles, their carrier surface can be designed and modified within a reasonable range as needed to change the relevant properties of the nanoparticles, such as drug loading capacity, drug release conditions, and biocompatibility [104]. From this, it can be seen that through their own properties and post-modification, nano-drug delivery systems can have excellent targeting capabilities, selectively exert effects on tumor cells, and avoid harm to normal cells in other parts of the body.

Metal-organic frameworks (MOFs) are crystalline hybrids built from metal nodes and organic linkers. Their ultra-high surface areas, tailorable pores and inherent biodegradability set them apart from conventional polymers, enabling uses that span gas storage, catalysis, functional materials design and, increasingly, theranostic nanomedicine. In oncology they serve mainly to:

Application in tumor multi-mode imaging

Today, MRI and CT remain the workhorses of clinical tumor imaging, yet each falls short: MRI delivers excellent soft-tissue contrast but its sensitivity is modest, whereas CT offers high spatial resolution but limited discrimination of soft-tissue lesions. CT can accurately present the three-body structure details of biological tissues but has low sensitivity to soft tissues. Metal-organic framework structures can be designed and prepared into multi-modal carriers through reasonable design, breaking through the shortcomings of single mode and improving the accuracy of tumor identification and diagnosis. Wang et al. synthesized and prepared a carrier capable of multi-mode imaging. Firstly, the ligand Ru has red fluorescence. Secondly, the synthesized Gd has a magnetic resonance response. Finally, the central ion Yb has X-ray attenuation. This carrier integrates fluorescence imaging, MRI, and CT, with high sensitivity, deep penetration, and good three-dimensional spatial resolution.

Application in tumor treatment

Metal-organic frameworks have excellent drug loading capacity, stable chemical structure, and high biocompatibility. They can selectively enrich in tumor tissues through the EPR effect and further control drug release by modifying the metal-organic framework with tumor-targeting small molecules, enhancing selective drug release and therapeutic effects, and reducing toxic side effects on normal tissues of the body. A single tumor treatment method often has limitations. Therefore, combining multiple modes of tumor treatment methods will be more effective and can avoid the toxic side effects caused by high doses of a single drug.

Application in integrated tumor diagnosis and treatment

Combining tumor treatment and diagnosis can achieve the inhibition of tumor growth during early diagnosis. Wang et al. used MIL-100(Fe) as the core and Fe_3O_4@C with magnetic targeting ability as the coating shell to load the drug DHA. The embedded small carbon dots in the middle carbon layer can serve as TPFI developers. DHA, as an anti-tumor drug, is controlled and released to treat cancer. This nanoparticle has dual modes of tumor imaging and treatment.

ZIF-8, a framework built from Zn^{2+} and 2-methylimidazole, degrades in a pH-selective manner—an attribute that makes it especially attractive for triggered drug delivery. ZIF-8 can remain structurally stable under neutral or alkaline conditions but specifically degrades under the slightly acidic pH conditions of the tumor microenvironment (TME), causing structural collapse and releasing the loaded drugs to the tumor site, ensuring the smooth transportation of the loaded drugs; high specific surface area and porosity can ensure high drug loading efficiency, greatly avoiding waste during the drug loading process; Zn^{2+} and methylimidazole are metabolized and degraded in the body without producing elements harmful to the human body. These advantages make ZIF-8 increasingly valued in drug delivery for treating tumors and other diseases. Currently, there are two main methods to load target drugs into ZIF-8 carriers: (1) using an immersion method to encapsulate drugs, mainly for drugs whose size does not exceed the pore size of ZIF-8. However, the drug transport system using this method to encapsulate drugs is prone to premature release of the target drug during cleaning and intravenous injection, causing waste of the drug and increasing the probability of toxic effects on normal tissue cells; (2) using in-situ drug encapsulation. Using this method to load drugs into ZIF-8 can solve the shortcomings of the previous method. Currently, small molecules such as DOX, curcumin, and caffeine have been successfully encapsulated in situ. They can form interactions with ZIF-8 and be successfully encapsulated into the ZIF-8 carrier. In addition, proteins or enzymes that are easily inactivated can be encapsulated into the ZIF-8 carrier to ensure the biological activity of the proteins or enzymes and better exert the efficacy of the drug.

Glucose oxidase (GOx) is an oxidoreductase. In the presence of O_2, GOx converts glucose into gluconic acid and H_2O_2, consuming both glucose and oxygen while the generated acid drops the tumor micro-environmental pH. Based on this, tumor treatment strategies for GOx have also been developed: (1) Tumor cell growth and metabolism rely on glucose. GOx consumes glucose, thereby affecting energy supply and starving them to death; (2) The generation of gluconic acid lowers the pH level in the TME, thereby triggering the sustained release of drugs from pH-responsive carriers; (3) The reduction of oxygen exacerbates the hypoxic environment of the tumor, and the increase in tumor hypoxia levels can be used to activate hypoxia-sensitive prodrugs, achieving effective chemotherapy; (4) The reaction product H_2O_2 is further converted into •OH through the Fenton reaction, significantly increasing intratumoral oxidative stress, thereby effectively eliminating tumors. Therefore, GOx can be combined with other enzymes, hypoxia-activated prodrugs, or Fenton reagents to produce synergistic cancer treatment.

Artemisinin is derived from the composite plant Artemisia annua. Dihydroartemisinin (DHA), as a first-generation derivative, has the molecular formula $C_{15}H_{24}O_5$ and a molecular weight of 284.35. DHA contains an endoperoxide bridge, which can be catalyzed by Fe(II) and produce free radicals [89]. Compared with normal cells, cancer cells often show higher dependence on high iron levels. This phenomenon gives DHA a certain selective ability to kill cancer cells. Data show that DHA can produce anti-tumor activity by inducing cell cycle arrest or apoptosis, preventing tumor angiogenesis, and inhibiting tumor invasion and metastasis. In addition, DHA has no significant killing effect on normal cells, indicating that DHA is a potential ideal anticancer drug.

Tirapazamine (TPZ), a clinical benzotriazine prodrug, is selectively lethal under hypoxia: in normoxic tissue its short-lived oxidizing radical is quenched by O_2 and the parent drug is regenerated, whereas in low-O_2 tumors the radical abstracts a proton from the C4′ of DNA ribose, then oxidizes the resulting DNA radical to produce lethal strand breaks.Therefore, TPZ has greater selective cytotoxicity to hypoxic cells in culture and hypoxic cells in tumors. Preclinical studies have shown that the combination of TPZ with other chemotherapy drugs can enhance activity. Phase II/III trials in melanoma and NSCLC show TPZ plus cisplatin outperforms either agent alone.

4.3 Limitations of CD-MOF as a Drug Carrier and Solutions

In addition to suitable morphology and size and low toxicity, drug carriers also need to have good stability [25]. Yet CD-MOF's inherent brittleness and rapid dissolution in aqueous environments erode its structural integrity en route to target sites, a drawback that has severely curtailed its biomedical utility. In recent years, to achieve CD-MOF as a drug delivery carrier, a lot of research has been carried out on how to effectively solve the stability of CD-MOF.

4.3.1 Crosslinking Free Hydroxyl Groups and Weak Interactions in CD-MOF

Chemical crosslinking is an effective way to maintain structural stability. Furukawa et al. used ethylene glycol diglycidyl ether's epoxy groups to crosslink adjacent free hydroxyl groups on CD-MOF. After crosslinking, the CD-MOF soaked in water lost potassium ions and transformed into porous cubic gel particles (CGP) similar in shape and size to CD-MOF. CGP retains CD-MOF's assets while overcoming its fragility, thereby unlocking the framework's full potential as a drug-delivery vehicle.However, it should be pointed out that this crosslinking reaction step is cumbersome and time-consuming. In addition, it takes a lot of time to remove the excess crosslinking agent in the reaction after synthesis. Inspired by this work, Singh et al. used diphenyl carbonate as a crosslinking agent and, under the catalysis of triethylamine, reacted with CD-MOF for only 4 hours to obtain nano- and micro-sized cubic structure CD-Cubes stable in water. Subsequently, the CD-Cubes prepared by this method were proved to successfully load doxorubicin hydrochloride (DOX). BET analysis gave nano CD-Cubes a surface area of 315 $m^2 g^{-1}$ and pore volume of 0.145 $cm^3 g^{-1}$; these pores adsorb 60–80 mg DOX per gram—eight-fold higher than directly cross-linked β-CD networks. Based on previous studies, we used 3,3'-dithiodipropionyl chloride to crosslink the free hydroxyl groups on CD-MOF. This reaction process is simple and rapid, and ssCGP stable in water can be obtained in 2 hours. The disulfide bond in ssCGP can be reduced to thiol by glutathione (GSH) and broken, causing the carrier to collapse. Therefore, after loading DOX, DOx@ssCGP can release a large amount of DOX in tumor cells with overexpression of GSH, achieving intelligent drug delivery.

Cross-linked CD-MOF keeps its uniform shape and high porosity, while simple water-washing removes surplus metal ions, eliminating potential toxicity. Moreover, the originally fixed pore size can be widened or narrowed by choosing linkers of different lengths, enlarging the spectrum of loadable drugs. Still, the cross-linking route is not without drawbacks.Crosslinking will make CD-MOF lose its original crystal structure, and the internal structure will change from ordered to disordered. The crosslinking agent will also occupy part of the pores, limiting the loading of macromolecular drugs, and may even reduce the drug loading capacity. After the crosslinked cubic particles disintegrate in the body, the free crosslinking agent is released, which may bring new potential toxicity. Therefore, in future work, finding suitable natural or commonly used pharmaceutical excipient molecules as crosslinking agents needs further study.

4.3.2 Loading Hydrophobic Contents

In addition to chemical modification, physical loading can also be used to provide a waterproof layer for CD-MOF to improve its stability in aqueous environments. Studies have shown that when hydrophobic macromolecules fully occupy the pores of CD-MOF, they can hinder the invasion of water molecules into the interior of CD-MOF. Based on this, Li incubated C_{60} with CD-MOF. C_{60} occupies the hydrophobic cavity of CD, and the C_{60}@CD-MOF complex is obtained. The addition of C_{60} does not affect the structure of CD-MOF but gives CD-MOF a certain hydrophobicity. The rich pores of C_{60}@CD-MOF can also be used to load the hydrophilic drug DOX, which has a certain sustained release effect. Compared with the crosslinking method, the physical embedding method is simpler and more effective, and the compound molecules are evenly distributed in CD-MOF, still maintaining a highly ordered structure. Yet this strategy only modestly enhances CD-MOF stability, leaving considerable room for further improvement. As the soaking time in the water environment 延长, C_{60}@CD-MOF will gradually disintegrate. In addition, the introduction of C_{60} reduces the drug loading capacity of CD-MOF. The crosslinking method product reaches equilibrium in a few minutes of drug loading, while C_{60}@CD-MOF needs to be soaked in the drug-containing solution for 48 hours. Possibly, C_{60} guests fill γ-CD cavities, shrinking pore volume and aperture, while their hydrophobic surface hampers aqueous DOX from diffusing into the framework.

4.3.3 Surface Modification of CD-MOF

Studies have shown that surface modification can also build a waterproof layer for CD-MOF, preventing water molecules from entering CD-MOF, which can be effectively used to stabilize CD-MOF. Singh et al. successfully modified a layer of cholesterol (CHS) on the surface of CD-MOF through chemical modification. The results showed that cholesterol-modified CD-MOF could not only effectively maintain its stability in water but also promote cell uptake to a certain extent. Pharmacokinetic studies found that the half-life of DOX loaded in CD-MOF-CHS could be extended by 4 times. Compared with the crosslinking method and physical embedding method, after modifying CHS, CD-MOF is stable in water without affecting its crystallinity and internal pores. However, it should be noted that surface modification greatly reduces the BET surface area of the system.

Moreover, since the modification only occurs on the surface, once the hydrophobic layer is damaged, the structure will collapse. As water molecules gradually penetrate, the CD-MOF structure will be gradually eroded..

4.3.4 Preparation of CD-MOF into Composite Microspheres

Using the biocompatible polymer polyacrylic acid (PAA) as the skeleton material, CD-MOF/PAA composite microspheres containing monodisperse CD-MOF can be prepared by oil/oil/solid emulsification solvent evaporation method. The microspheres can effectively increase the stability of the internal CD-MOF in water-based media. The CD-MOF internally loaded with two drugs, ibuprofen and lansoprazole, improves the stability and solubility of drug molecules, can effectively avoid the burst release of microspheres, achieve sustained drug release, and reduce the cytotoxicity of the carrier. However, the microspheres prepared by this method have a large particle size (50-100 nm) and carry the risk of organic solvent residue.

5. Future Directions

The exploration of Metal-Organic Frameworks (MOFs) in biomedical applications, particularly as drug carriers, has transitioned from a nascent curiosity to a burgeoning frontier in materials science and nanomedicine over the past two decades. The remarkable progress achieved thus far is undeniable: researchers have successfully demonstrated the high loading capacity of MOFs for a vast array of therapeutic agents (from small-molecule chemotherapeutics to large biomacromolecules like proteins and nucleic acids), engineered sophisticated stimuli-responsive release mechanisms, and developed multifunctional platforms that combine drug delivery with imaging, sensing, and therapeutic modalities. The intrinsic porosity, unparalleled surface area, synthetic tunability, and biodegradable nature of many MOFs position them as superior candidates compared to traditional nanocarriers like liposomes, polymers, and mesoporous silica. However, as the field matures from proof-of-concept studies to pre-clinical and, eventually, clinical translation, the focus must shift from merely showcasing potential to systematically addressing the formidable challenges that lie ahead. The future outlook for MOF-based drug carriers is exceptionally promising but hinges on strategic advancements across several critical axes: (1) enhancing biocompatibility and elucidating long-term biosafety, (2) advancing synthesis and scale-up for Good Manufacturing Practice (GMP) compliance, (3) engineering sophisticated multifunctional and "smart" systems, and (4) navigating the complex pathway of clinical translation and regulatory approval.

1. The Biocompatibility and Biosafety Imperative: From Acute Toxicity to Long-Term Fate

The foremost and non-negotiable requirement for any material intended for human use is safety. Early research often prioritized high drug loading and novel functionality, sometimes overlooking comprehensive toxicological assessment. The future of MOF-DDS depends on a deep, mechanistic understanding of their biocompatibility and long-term fate within the body. a) Material Selection and Degradation Profiling: A significant trend is the move towards components with established safety profiles. The use of endogenous or essential metal ions (e.g., Fe^{2+}/Fe^{3+}, Zn^{2+}, Mg^{2+}, Ca^{2+}) and linkers that are biologically benign or metabolites (e.g., fumarate, citrate, amino acids) is paramount. The degradation products of MOFs must be meticulously characterized. For instance, iron-carboxylate MOFs like MIL-100(Fe) degrade into iron ions (which can be metabolized by the body's natural stores) and organic linkers, presenting a favorable toxicity profile. Future research must establish comprehensive "degradation libraries" for a wide range of MOFs, correlating their structures with the nature, kinetics, and biological impact of their breakdown products. This will allow for the rational design of MOFs with predictable and safe metabolic pathways. b) Immunogenicity and Long-Term Accumulation: While many MOFs show low acute toxicity in cell cultures and short-term animal studies, the consequences of chronic exposure and long-term accumulation in reticuloendothelial system (RES) organs like the liver and spleen require intensive investigation. Key questions remain: Do certain MOF structures induce unintended immunogenic responses or chronic inflammation? How does repeated dosing affect organ function over months or years? Advanced in vitro models (e.g., 3D organoids, immune cell co-cultures) and long-term in vivo studies are essential to answer these questions. Surface engineering with stealth coatings like polyethylene glycol (PEG) can reduce opsonization and RES uptake, but the immunogenicity of PEG itself (the phenomenon of anti-PEG antibodies) is a growing concern, prompting the exploration of alternative coatings like zwitterionic lipids or polysaccharides. c) Standardization of Toxicity Assessment: The field would benefit immensely from standardized protocols for evaluating MOF

toxicity. Factors such as batch-to-batch consistency, thorough characterization (size, zeta potential, porosity) before biological testing, and the use of relevant disease models are crucial for generating reliable and comparable data across different research groups. This standardization is a prerequisite for meaningful meta-analyses and for building a robust database that informs safe-by-design principles.

2. Scaling Up and Mastering Manufacturing: The Bridge from Lab Bench to Bedside

The sophisticated multi-step syntheses that produce gram-scale quantities of high-quality MOFs in a research laboratory are often impractical and economically unviable for industrial-scale production. Bridging this scale-up gap is a monumental but essential engineering challenge. a) Green and Scalable Synthesis: Current synthesis methods frequently rely on organic solvents like dimethylformamide (DMF) or N,N-Diethylformamide (DEF), which are toxic and environmentally hazardous, requiring extensive purification steps. The future lies in developing sustainable synthetic routes. This includes: Aqueous-Phase Synthesis: Designing MOFs that can be synthesized stably and with high crystallinity in water. Mechanochemical Synthesis: Using ball-milling techniques that are solvent-free, rapid, and scalable. Continuous Flow Synthesis: Moving from batch reactions to continuous flow reactors, which offer better control over parameters (temperature, pressure, mixing), improved reproducibility, and inherent scalability for industrial production. Microwave and Ultrasound-Assisted Synthesis: These energy-efficient methods can drastically reduce reaction times and improve yields. The goal is to develop processes that are not only scalable but also align with Green Chemistry principles, minimizing waste and energy consumption, which is critical for cost-effectiveness and environmental sustainability. b) Achieving Robust Quality Control (QC): For pharmaceutical applications, batch-to-batch reproducibility is non-negotiable. Minor variations in synthesis can lead to differences in particle size, surface charge, defect density, and ultimately, drug loading and release kinetics. Implementing rigorous Quality by Design (QbD) principles will be essential. This involves identifying Critical Quality Attributes (CQAs) of the MOF (e.g., size distribution, crystalline purity, surface chemistry) and understanding how Critical Process Parameters (CPPs) during synthesis affect them. Advanced in-line and on-line process analytical technologies (PAT) will be needed to monitor synthesis in real-time, ensuring every batch meets stringent specifications for pharmaceutical use. c) Post-Synthetic Functionalization and Drug Loading at Scale: The processes for loading drugs into the MOF pores and functionalizing the surface with targeting ligands must also be scalable. Efficient, one-pot synthesis and loading strategies are highly desirable. Techniques for consistent and quantitative conjugation of antibodies, peptides, or other targeting moieties need to be developed for large batches without compromising the biological activity of the ligands.

3. The Rise of Intelligent and Multifunctional Theranostic Platforms

The true potential of MOFs extends far beyond being simple drug containers. Their unique chemistry allows them to be engineered as "smart" theranostic (therapy + diagnosis) platforms that can diagnose, deliver therapy, and monitor response in real-time. a) Advanced Stimuli-Responsiveness: While pH-responsive release for targeting the tumor microenvironment is well-established, future systems will exploit a wider range of endogenous and exogenous stimuli with greater specificity. Enzyme-Responsive MOFs: Designing linkers that are specific substrates for enzymes overexpressed in diseases (e.g., matrix metalloproteinases in cancer, or cathepsins in inflammation). This provides a highly specific release trigger. Redox-Responsive MOFs: Utilizing linkers with disulfide bonds that are cleaved in the high glutathione (GSH) concentrations of cancer cells. Exogenous Stimuli with Deep-Tissue Penetration: Near-Infrared (NIR) light, magnetic fields, and ultrasound can be used to trigger drug release non-invasively and with high spatiotemporal control. For example, upconversion nanoparticles (UCNPs) can be encapsulated within MOFs to convert deep-tissue-penetrating NIR light into higher-energy UV/vis light, which then triggers cargo release from a photosensitive MOF shell. b) Integration with Other Nanotechnologies (Hybrid Systems): The future will see more MOF-hybrid systems that combine the strengths of different nanomaterials. MOF-in-Lipid/Polymer Composites: Encapsulating MOF nanoparticles within liposomes or biodegradable polymer shells can enhance stability in biological fluids, provide an additional diffusion barrier for controlled release, and allow for easier surface functionalization. MOF-Coated Implants or Stents: Coating medical devices with drug-eluting MOF films for localized and sustained therapy, such as anti-inflammatory drugs on bone implants or anticoagulants on vascular stents. Core-Shell Structures: Creating structures with a MOF shell around a functional core (e.g., a magnetic nanoparticle for MRI contrast and magnetic hyperthermia, or a gold nanorod for photothermal therapy) and vice versa. c) Theranostics and Real-Time Monitoring: The ability to incorporate imaging agents (e.g., Gd^{3+} for MRI, Zr^{4+} for PET, fluorescent linkers

for optical imaging) directly into the MOF scaffold is a powerful advantage. The next generation will focus on "active" theranostics, where the MOF not only images the target site but also reports on the therapeutic action. For instance, a MOF could be designed to change its MRI signal or fluorescence intensity upon releasing its drug payload, providing direct feedback on treatment efficacy. d) Expanding the Therapeutic Cargo Scope: Research will continue to move beyond small molecules to more complex biologics. Gene Therapy: MOFs show great promise for delivering fragile nucleic acids (DNA, siRNA, miRNA). Their porous structure can protect these molecules from nuclease degradation. Future work will focus on improving transfection efficiency and developing nuclear-localizing MOF vectors. Protein and Enzyme Delivery: The large pores of some MOFs (e.g., those of the NU-1000 or PCN-333 family) can encapsulate large enzymes, protecting them while allowing substrate diffusion. This opens avenues for enzyme replacement therapies or intracellular catalytic reactions.

6. Conclusion

CD-MOF has good biocompatibility, can load a variety of drug molecules, and shows great potential in the field of drug delivery. Methods such as crosslinking, loading hydrophobic substances, surface modification, and preparing composite microspheres can effectively increase the stability of CD-MOF. Developing more effective and simpler strategies to stabilize CD-MOF in water environments to regulate drug release can further expand the potential applications of CD-MOF. In addition, finding drug molecules with diagnostic and therapeutic functions to stabilize CD-MOF and simultaneously load other drug molecules to achieve combined medication or integrated diagnosis and treatment will be a very meaningful work. With the continuous deepening of research on CD-MOF, it is believed that CD-MOF will play more roles in the biomedical field in the future.

References

[1]
[2] P. SCHELTENS, B. DE STROOPER, M. KIVIPELTO, et al. Alzheimer's disease. The Lancet, 2021,397(10284): 1 577-1590
[3] M. A. DETURE, D. W. DICKSON. The neuropathological diagnosis of Alzheimers disease. Molecular Neurod egeneration, 2019, 14(1): 1-18
[4] L. F. JIA, Y.F. DU, L. CHU, et al. Prevalence, risk factors, and management of dementia and mildcognitive i mpairment in adults aged 60 years or older in China: a cross-sectional study. The Lancet Public Health, 20 20, 5(12): 661-671
[5] J. HARDY, D. J. SELKOE. The amyloid hypothesis of Alzheimer's disease: progress and problems on the roa d to therapeutics. Science, 2002, 297(5580): 353-356
[6] C. L. YUAN, X. L. GUO, Q. F. ZHOU, et al. OAB-14, a bexarotene derivative, improves Alzheimer's disease-re lated pathologies and cognitive impairments by increasing β-amyloid clearance in APP/PS1 mice. Biochimi ca et Biophysica Acta (BBA)-Molecular Basis of Disease, 2019, 1865(1): 161-180
[7] H. A. ALHAZMI, M. ALBRATTY. An update on the novel and approved drugs for Alzheimer
[8] disease. Saudi Pharmaceutical Journal, 2022, 30(12): 1755-1764
[9] X. LIU, B. Y. SUI, J. SUN. Blood-brain barrier dysfunction induced by silica NPs in vitro and in vivo : involve ment of oxidative stress and Rho-kinase/JNK signaling pathways. Biomaterials, 2017, 121: 64-82
[10] K. T. NGUYEN, M. N. PHAM, T. V. VO, et al. Strategies of engineering nanoparticles for treating neurodege nerative disorders. Current Drug Metabolism, 2017, 18(9): 786-797
[11] D. FURTADO, M. BJÖRNMALM, S. AYTON, et al. Overcoming the blood-brain barrier: the role of nanomate rials in treating neurological diseases. Advanced Materials, 2018, 30(46): 1801362
[12] H. SUNG, J. FERLAY, R. L. SIEGEL, et al. Global cancer ctatistics 2020: GLOBOCAN estimates of incidence an d mortality worldwide for 36 cancers in 185 countries. CA: A Cancer Journal for Clinicians, 2021, 71(3): 20 9-249
[13] J. FERLAY, M. COLOMBET, I. SOERJOMATARAM, et al. Cancer statistics for the year 2020: an overview. Int ernational Journal of Cancer, 2021, 149(4): 778-789
[14] J. L. LI, L. JIANG, B. W. WANG, et al. Significant differences in biological activity of mononuclear Cu(II) and Ni(II) complexes with the polyquinolinyl ligand. New Journal of Chemistry, 2015, 39(1): 529-538
[15] W. XIAO, X. ZENG, H. LIN, et al. Dual stimuli-responsive multi-drug delivery system for the individually con trolled release of anti-cancer drugs. Chemical Communications, 2015, 51(8): 1475- 1478

[16] H. G. QIN, S. ZHAO, H. P. GONG, et al. Recent progress in the application of metal organic frameworks in surface-enhanced raman scattering detection. Biosensors, 2023, 13(4): 479
[17] B F. HOSKINS, R. ROBSON. Infinite polymeric frameworks consisting of three dimensionally linked rod-like segments. J Am Chem Soc, 2002, 111(15): 5962-5964
[18] J. J. PERRY Ⅳ, J. A. PERMAN, M. J. ZAWOROTKO. Design and synthesis of metal-organic frameworks using metal-organic polyhedra as supermolecular building blocks. Chemical Society Reviews, 2009, 38(5):1400-1417
[19] F. SCHRÖDER, D. ESKEN, M. COKOJA, et al. Ruthenium nanoparticles inside porous [Zn4O(bdc)3] by hydrogenolysis of adsorbed [Ru(cod)(cot)]: a solid-state reference system for surfactant-stabilized ruthenium colloids. Journal of the American Chemical Society, 2008, 130(19): 6119-6130
[20] N. A. H. M. NORDIN, A. F. ISMAIL, A. MUSTAFA, et al. Aqueous room temperature synthesis of zeolitic imidazole framework 8 (ZIF-8) with various concentrations of triethylamine. RSC Advances, 2014, 4(63): 33292-33300
[21] K. LI, S. L. LIN, Y. S. LI, et al. Aqueous-phase synthesis of mesoporous Zr-based MOFs templated by amphoteric surfactants. Angewandte Chemie International Edition, 2018, 57(13): 3439-3443
[22] J. CRAVILLON, R. NAYUK, S. SPRINGER, et al. Controlling zeolitic imidazolate framework nano- and microcrystal formation: insight into crystal growth by time-resolved in situ static light scattering. Chemistry of Materials, 2011, 23(8): 2130-2141
[23] S. KOUSER, A. HEZAM, M. J. N. KHADRI, et al. A review on zeolite imidazole frameworks: synthesis, properties, and applications. Journal of Porous Materials, 2022, 29(3): 663-681
[24] J. ZHANG, T. WU, C. ZHOU, et al. Zeolitic boron imidazolate frameworks. Angewandte Chemie International Edition, 2009, 48(14): 2542-2545
[25] PHAN, C. J. DOONAN, F. J. URIBE-ROMO, et al. Synthesis, structure, and carbon dioxide capture properties of zeolitic imidazolate frameworks. Accounts of chemical research, 2010, 43(1): 58-67
[26] R. AHMAD, U. A. KHAN, N. IQBAL, et al.Zeolitic imidazolate framework(ZIF)-derived porous carban materials for supercapacitors: an overview. RSC Advances, 2020, 10(71): 43733-43750
[27] X. F. MENG, J. W.GUAN, S. S. LAI, et al. pH-responsive curcumin-based nanoscale ZIF-8 combining chemophotodynamic therapy for excellent antibacterial activity. RSC Advances, 2022, 12(16): 10005-10013
[28] K. S. PARK, Z. NI, A P. CÔTÉ, et al. Exceptional chemical and thermal stability of zeolitic imidazolate frameworks. Proceedings of the National Academy of Sciences of the United States of America, 2006, 103(27): 10186-10191
[29] M. L. ZHOU, T. F. TANG, D. F. QIN, et al. Hematite nanoparticle decorated MIL-100 for the highly selective and sensitive electrochemical detection of trace-level paraquat in milk and honey. Sensors and Actuators B: Chemical, 2023, 376: 132931
[30] BOUTIN, S. COUCK, F-X. COUDERT, et al. Thermodynamic analysis of the breathing of amino-functionalized MIL-53(Al) upon CO2 adsorption. Microporous and Mesoporous Materials, 2010, 140(1): 108-113
[31] G. HAN, K. M. RODRIGUEZ, Q. H. QIAN, et al. Acid-modulated synthesis of high surface area amine-functionalized MIL-101(Cr) nanoparticles for CO2 separations. Industrial & Engineering Chemistry Research, 2020, 59(40): 18139-18150
[32] P. HORCAJADA, T. CHALATI, C. SERRE, et al. Porous metal-organic-framework nanoscale carriers as a potential platform for drug delivery and imaging. Nature Materials, 2009, 9(2): 172- 178
[33] J. H. CAVKA, S. JAKOBSEN, U. OLSBYE, et al. A new zirconium inorganic building brick forming metal organic frameworks with exceptional stability. Journal of the American Chemical Society, 2008, 130(42): 13850-13851
[34] S. S. WANG, G. B. ZHOU, Y. H. SUN, et al. A computational study of water in UiO-66 Zr-MOFs: diffusion, hydrogen bonding network, and confinement effect. AIChE Journal, 2020, 67(3): e17035
[35] Y. FENG, Q. CHEN, M. Q. JIANG, et al. Tailoring the properties of UiO-66 through defect engineering: a review. Industrial & Engineering Chemistry Research, 2019, 58(38): 17646-17659
[36] C. G. PISCOPO, A. POLYZOIDIS, M. SCHWARZER, et al. Stability of UiO-66 under acidic treatment: opportunities and limitations for post-synthetic modifications. Microporous and Mesoporous Materials, 2015, 208: 30-35
[37] X. C. GAO, R. X. CUI, G. F. JI, et al. Size and surface controllable metal-organic frameworks (MOFs) for fluorescence imaging and cancer therapy. Nanoscale, 2018, 10(13): 6205-6211

[38] J. HE, F. J. XU, Y. F. TIAN, et al. Atmospheric low-temperature plasma for direct post-synthetic modificatio n of UiO-66. Chemical Communications, 2020, 56(43): 5803-5806
[39] H. L. LI, M. EDDAOUDI, M. O'KEEFFE, et al. Design and synthesis of an exceptionally stable and highly poro us metal-organic framework. Nature, 1999, 402(6759): 276-279
[40] N. M. RODRIGUES, J. B. L. MARTINS. Theoretical evaluation of the performance of IRMOFs and M-MOF-74 in the formation of 5-fluorouracil@MOF. RSC Advances, 2021, 11(49): 31090- 31097
[41] M. EDDAOUDI, J. KIM, N. ROSI, et al. Systematic design of pore size and functionality in isoreticular MOFs and their application in methane storage. Science, 2002, 295(5554): 469-472
[42] M. R. CAI, L. Y. QIN, L. N. PANG, et al. Amino-functionalized Zn metal organic frameworks as antitumor dr ug curcumin carriers. New Journal of Chemistry, 2020, 44(41): 17693-17704
[43] S. S.-Y. CHUI, A. M.-F. LO, J. P. H. CHARMANT, et al. A chemically functionalizable nanoporous material [Cu 3(TMA)2(H2O)3]n.Science, 1999, 283(5405): 1148-1150
[44] K-S. LIN, A. K. ADHIKARI, C-N. KU, et al. Synthesis and characterization of porous HKUST-1 metal organic fr ameworks for hydrogen storage. International Journal of Hydrogen Energy, 2012, 37(18): 13865-13871
[45] W. J. XUE, Z. Q. ZHANG, H. L. HUANG, et al. Theoretical insights into the initial hydrolytic breakdown of HK UST-1. The Journal of Physical Chemistry C, 2019, 124(3): 1991-2001
[46] S. KITAGAWA, R. MATSUDA. Chemistry of coordination space of porous coordination polymers. Coordinat ion Chemistry Reviews, 2007, 251(21-24): 2490-2509
[47] Y. W. CHEN, Z. W. QIAO, D. F. LV, et al. Efficient adsorptive separation of C3H6 over C3H8 on flexible and t hermoresponsive CPL-1. Chemical Engineering Journal, 2017, 328: 360-367
[48] G. Q. KONG, Z. D. HAN, Y. B. HE, et al. Expanded organic building units for the construction of highly porou s metal-organic frameworks. Chemistry-A European Journal, 2013, 19(44): 14886- 14894
[49] D. YUE, Y. K. HUANG, J. ZHANG, et al. Two-dimensional metal-organic framework as fluorescent probe for ascorbic acid sensing. European Journal of Inorganic Chemistry, 2018, 2018(2): 173-177
[50] J. Y. PEI, K. SHAO, J. X. WANG, et al. A chemically stable hofmann-type metal-organic framework with san dwich-like binding sites for benchmark acetylene capture. Advanced Materials, 2020, 32(24): 1908257
[51] T. F. XIA, Y. T. WAN, Y. P. LI, et al. Highly stable lanthanide metal-organic framework as an internal calibrat ed luminescent sensor for glutamic acid, a neuropathy biomarker. Inorganic Chemistry, 2020, 59(13): 880 9-8817
[52] S. SINGH, S. KAUSHAL, J. KAUR, et al. CaFu MOF as an efficient adsorbent for simultaneous removal of imi dacloprid pesticide and cadmium ions from wastewater. Chemosphere, 2021, 272: 129648
[53] YURDUŞEN, Y. YÜRÜM. A controlled synthesis strategy to enhance the CO2 adsorption capacity of MIL-88 B type MOF crystallites by the crucial role of narrow micropores. Industrial & Engineering Chemistry Rese arch, 2019, 58(31): 14058-14072
[54] F. NOROUZI, H. R. KHAVASI. Diversity-oriented metal decoration on UiO-type metal-organic frameworks: an efficient approach to increase CO2 uptake and catalytic conversion to cyclic carbonates. ACS Omega, 2 019, 4(21): 19037-19045 [
[55] Y. N. GONG, J. H. MEI, J. W. LIU, et al. Manipulating metal oxidation state over ultrastable metal-organic fr ameworks for boosting photocatalysis. Applied Catalysis B: Environmental, 2021, 292: 120156
[56] M. NIE, H. SUN, D. LEI, et al. Novel Pd/MOF electrocatalyst for hydrogen evolution reaction. Materials Che mistry and Physics, 2020, 254: 123481
[57] BIENIEK, A. P. TERZYK, M. WIŚNIEWSKI, et al. MOF materials as therapeutic agents, drug carriers, imaging agents and biosensors in cancer biomedicine: recent advances and perspectives. Progress in Materials Sci ence, 2021, 117: 100743
[58] Q. Y. QIN, M. YANG, Y. SHI, et al. Mn-doped Ti-based MOFs for magnetic resonance imagingguided synerg istic microwave thermal and microwave dynamic therapy of liver cancer. Bioactive Materials, 2023, 27: 72 -81
[59] J. CAO, X. J. LI, H. Q. TIAN. Metal-organic framework (MOF)-based drug delivery. Current Medicinal Chemi stry, 2020, 27(35): 5949-5969
[60] X. MI, M. G. HU, M. R. DONG, et al. Folic acid decorated zeolitic imidazolate framework (ZIF- 8) loaded wit h baicalin as a nano-drug delivery system for breast cancer therapy. International Journal of Nanomedicin e, 2021, 16: 8337-8352
[61] J. H. ZHAO, F. C. YIN, L. M. JI, et al. Development of a tau-targeted drug delivery system using a multifunct ional nanoscale metal-organic framework for Alzheimer's disease therapy. ACS Applied Materials & Interf aces, 2020, 12(40): 44447-44458

[62] Y. X. SONG, S. Y. LU, S. H. SUN, et al. A fluorometric and optical signal dual-readout detection of alkaline phosphatase activity in living cells based on ATP-mediated porphyrin MOFs. Sensors and Actuators B: Chemical, 2021, 342: 130017
[63] C. Y. WANG, C. C. WANG, X. W. ZHANG, et al. A new Eu-MOF for ratiometrically fluorescent detection toward quinolone antibiotics and selective detection toward tetracycline antibiotics. Chinese Chemical Letters, 2022, 33(3): 1353-1357
[64] T. M. ALLEN, P. R. CULLIS. Liposomal drug delivery systems: from concept to clinical applications. Advanced Drug Delivery Reviews, 2013, 65(1): 36-48
[65] G. GREGORIADIS, B. E. RYMAN. Liposomes as carriers of Enzymes or drugs: a new approach to the treatment of storage diseases. Biochemical journal, 1971, 124(5): 58P
[66] E. RIDEAU, R. DIMOVA, P. SCHWILLE, et al. Liposomes and polymersomes: a comparative review towards cell mimicking. Chemical Society Reviews, 2018, 47(23): 8572-8610
[67] E. YUBA. Development of functional liposomes by modification of stimuli-responsive materials and their biomedical applications. Journal of materials chemistry B, 2020, 8(6): 1093-1107
[68] Y. LI, T. J. JI, M. TORRE, et al. Aromatized liposomes for sustained drug delivery. Nature Communications, 2023, 14(1): 6659
[69] Z. J. CHEN, S. C. YANG, X. L. LIU, et al. Nanobowl-supported liposomes improve drug loading and delivery. Nano Letters, 2020, 20(6): 4177-4187
[70] C. DU, Y. LIANG, Q. M. MA, et al. Intracellular tracking of drug release from pH-sensitive polymeric nanoparticles via FRET for synergistic chemo-photodynamic therapy. Journal of Nanobiotechnology, 2019, 17(1): 1-18
[71] N. HUANG, S. LIU, X. G. LIU, et al. PLGA nanoparticles modified with a BBB-penetrating peptide co-delivering Aβ generation inhibitor and curcumin attenuate memory deficits and neuropathology in Alzheimer's disease mice. Oncotarget, 2017, 8(46): 81001-81013
[72] B. T. LU, X. K. LV, Y. LE. Chitosan-modified PLGA nanoparticles for control-released drug delivery. Polymers, 2019, 11(2): 304
[73] K. S. SIDDIQI, A. HUSEN. Recent advances in plant-mediated engineered gold nanoparticles and their application in biological system. Journal of Trace Elements in Medicine and Biology, 2017, 40: 10-23
[74] HUSEN. Gold nanoparticles from plant system: synthesis, characterization and their application. Nanoscience and Plant-Soil Systems. 2017: 455-479
[75] K. SIVAJI, R. R. KANNAN. Polysorbate 80 coated gold nanoparticle as a drug carrier for brain targeting in zebrafish model. Journal of Cluster Science, 2019, 30(4): 897-906
[76] Z. ZHANG, Y. H. JI. Mesoporous manganese dioxide coated gold nanorods as a multiresponsive nanoplatform for drug delivery. Industrial & Engineering Chemistry Research, 2019, 58(8): 2991-2999
[77] T. T. LI, S. X. SHI, S. GOEL, et al. Recent advancements in mesoporous silica nanoparticles towards therapeutic applications for cancer. Acta Biomaterialia, 2019, 89: 1-13
[78] E. NIEMELÄ, D. DESAI, R. NIEMI, et al. Nanoparticles carrying fingolimod and methotrexate enables targeted induction of apoptosis and immobilization of invasive thyroid cancer. European Journal of Pharmaceutics and Biopharmaceutics, 2020, 148: 1-9
[79] H. Y. TANG, D. XIANG, F. WANG, et al. 5-ASA-loaded SiO2 nanoparticles-a novel drug delivery system targeting therapy on ulcerative colitis in mice. Molecular Medicine Reports, 2017, 15(3): 1117-1122
[80] C. CHA, S. R. SHIN, N. ANNABI, et al. Carbon-based nanomaterials: multifunctional materials for biomedical engineering. ACS nano, 2013, 7(4): 2891-2897
[81] S. LOHAN, K. RAZA, S. MEHTA, et al. Anti-alzheimer's potential of berberine using surface decorated multi-walled carbon nanotubes: a preclinical evidence. International Journal of Pharmaceutics, 2017, 530(1-2): 263-278
[82] R. MALEKI, A. KHOSHOEI, E. GHASEMY, et al. Molecular insight into the smart functionalized TMC-fullerene nanocarrier in the pH-responsive adsorption and release of anticancer drugs. Journal of Molecular Graphics and Modelling, 2020, 100: 107660
[83] R. SINGH, B. KUMAR, R. K. SAHU, et al. Development of a pH-sensitive functionalized metal organic framework:in vitrostudy for simultaneous delivery of doxorubicin and cyclophosphamide in breast cancer. RSC Advances, 2021, 11(53): 33723-33733
[84] D. Q. YU, M. M. MA, Z.W. LIU, et al. MOF-encapsulated nanozyme enhanced siRNA combo: control neural stem cell differentiation and ameliorate cognitive impairments in Alzheimer's disease model. Biomaterials, 2020, 255: 120160

[85] S. N. LIU, C. L. HU, Y. LIU, et al. One-pot synthesis of DOX@covalent organic framework with enhanced ch emotherapeutic efficacy. Chemistry-A European Journal, 2019, 25(17): 4315-4319
[86] Y. T. JIA, L. N. ZHANG, B. N. HE, et al. 8-Hydroxyquinoline functionalized covalent organic framework as a pH sensitive carrier for drug delivery. Materials Science and Engineering: C, 2020, 117: 111243
[87] Z. Z. ,YANG Y. Q. ZHANG, Z. Z. WANG, et al. Enhanced brain distribution and pharmacodynamics of rivastig mine by liposomes following intranasal administration. International Journal of Pharmaceutics, 2013, 452 (1-2): 344-354
[88] S. A. JOSHI, S. S. CHAVHAN, K. K. SAWANT. Rivastigmine-loaded PLGA and PBCA nanoparticles: preparatio n, optimization, characterization, in vitro and pharmacodynamic studies. European Journal of Pharmaceut ics and Biopharmaceutics, 2010, 76(2): 189-199
[89] Z. YANG, Y. G. ZHANG, Y. L. YANG, et al. Pharmacological and toxicological target organelles and safe use of single-walled carbon nanotubes as drug carriers in treating Alzheimer disease. Nanomedicine: Nanotec hnology, Biology and Medicine, 2010, 6(3): 427-441
[90] M. J. KIM, S. U. REHMAN, F. U. AMIN, et al. Enhanced neuroprotection of anthocyanin-loaded PEG-gold n anoparticles against Aβ1-42-induced neuroinflammation and neurodegeneration via the NF-KB /JNK/GSK 3β signaling pathway. Nanomedicine: Nanotechnology, Biology and Medicine, 2017, 13(8): 2533-2544
[91] J. SANTOS, M. T. QUIMQUE, R. A. LIMAN, et al. Computational and experimental assessments of magnolol as a neuroprotective agent and utilization of UiO-66(Zr) as its drug delivery system. ACS Omega, 2021, 6 (38): 24382-24396
[92] S. J. LI, D. Q. ZHANG, S. H. SHENG, et al. Targeting thyroid cancer with acid-triggered release of doxorubici n from silicon dioxide nanoparticles. International Journal of Nanomedicine, 2017, 12: 5993-6003
[93] M. A. KHAN, M. ZAFARYAB, S. H. MEHDI, et al. Characterization and carboplatin loaded chitosan nanopart icles for the chemotherapy against breast cancer in vitro studies. International Journal of Biological Macro molecules, 2017, 97: 115-122
[94] S. A. LILA, M. S. SOLIMAN, H. C. KIRAN, et al. Tamoxifen-loaded functionalized graphene nanoribbons for breast cancer therapy. Journal of Drug Delivery Science and Technology, 2021, 63: 102499
[95] N. AMREDDY, A. BABU, J. PANNEERSELVAM, et al. Chemo-biologic combinatorial drug delivery using folat e receptor-targeted dendrimer nanoparticles for lung cancer treatment. Nanomedicine: Nanotechnology, Biology and Medicine, 2018, 14(2): 373-384
[96] V. GUPTA, S. MOHIYUDDIN, A. SACHDEV, et al. PEG functionalized zirconium dicarboxylate MOFs for doce taxel drug delivery in vitro. Journal of Drug Delivery Science and Technology, 2019, 52: 846-855
[97] X. L. GUO, X. F. BAO, X. J. WANG, et al. OAB-14 Effectively ameliorates the dysfunction of the endosomal-autophagic-lysosomal pathway in APP/PS1 transgenic mice. ACS Chemical Neuroscience, 2021, 12(21): 39 85-3993
[98] Y. N. WU, M. M. ZHOU, B. R. ZHANG, et al. Amino acid assisted templating synthesis of hierarchical zeoliti c imidazolate framework-8 for efficient arsenate removal. Nanoscale, 2014, 6(2):
[99] X. Q. CHENG, A. F. ZHANG, K. K. HOU, et al. Size- and morphology-controlled NH2-MIL- 53(Al) prepared in DMF-water mixed solvents. Dalton Transactions, 2013, 42(37): 13698
[100] M. L. CHEN, S. Y. ZHOU, Z. XU, et al. Metal-organic frameworks of MIL-100(Fe, Cr) and MIL-101(Cr) for aro matic amines adsorption from aqueous solutions. Molecules, 2019, 24(20): 3718
[101] Y. C. LIN, C. L. KONG, L. CHEN. Direct synthesis of amine-functionalized MIL-101(Cr) nanoparticles and app lication for CO2 capture. RSC Advances, 2012, 2(16): 6417-6419
[102] G. AKIYAMA, R. MATSUDA, H. SATO, et al. Cellulose hydrolysis by a new porous coordination polymer dec orated with sulfonic acid functional groups. Advanced Materials, 2011, 23(29): 3294-3297
[103] S. N. TAMBAT, P. K. SANE, S. SURESH, et al. Hydrothermal synthesis of NH2-UiO-66 and its application for adsorptive removal of dye. Advanced Powder Technology, 2018, 29(11): 2626-2632
[104] F. HABIMANA, D. SHI, S. H. JI. Synthesis of Cu-BTC/Mt composites porous materials and their performance in adsorptive desulfurization process. Applied Clay Science, 2018, 152: 303-310
[105] Q. MA, R. ZHANG. Facile synthesis of redox-responsive paclitaxel drug release platform using metal-organ ic frameworks (ZIF-8) for gastric cancer treatment. Materials Research Express, 2020, 7(9): 059402
[106] M. HE, J. F. YAO, Q. LIU, et al. Facile synthesis of zeolitic imidazolate framework-8 from a concentrated aq ueous solution. Microporous and Mesoporous Materials, 2014, 184: 55-60
[107] L. ZHOU, N. LI, G. OWENS, et al. Simultaneous removal of mixed contaminants, copper and norfloxacin, fr om aqueous solution by ZIF-8. Chemical Engineering Journal, 2019, 362: 628-637

[108] L. ZHOU, N. LI, X. Y. JIN, et al. A new nFe@ZIF-8 for the removal of Pb(II) from wastewater by selective ads orption and reduction. Journal of Colloid and Interface Science, 2020, 565: 167-176
[109] M. N. LI, P. SUN, Q. WU, et al. Core-shell magnetic metal-organic framework molecularly imprinted nanos pheres for specific adsorption of tetrabromobisphenol a from water. Environmental Science: Nano, 2018, 5(11): 2651-2662
[110] J. B. HUO, L. XU, J. C. E. YANG, et al. Magnetic responsive Fe3O4-ZIF-8 core-shell composites for efficient r emoval of As(III) from water. Colloids and Surfaces A: Physicochemical and Engineering Aspects, 2018, 53 9: 59-68
[111] C. LI, Z. H. XIONG, J. M. ZHANG, et al. The strengthening role of the amino group in metalorganic framewo rk MIL-53(Al) for methylene blue and malachite green dye adsorption. Journal of Chemical & Engineering Data, 2015, 60(11): 3414-3422
[112] Ş. S. BAYAZIT, S. T. DANALIOĞLU, M. A. SALAM, et al. Preparation of magnetic MIL- 101(Cr) for efficient re moval of ciprofloxacin. Environmental Science and Pollution Research, 2017, 24(32): 25452-25461
[113] P. C. HOU, G. J. XING, D. HAN, et al. MIL-101(Cr)/graphene hybrid aerogel used as a highly effective adsor bent for wastewater purification. Journal of Porous Materials, 2019, 26(6): 1607- 1618
[114] Z. B. LIU, B. H. ZHAO, L. Q. ZHU, et al. Performance of MIL-101(Cr)/water working pair adsorption refriger ation system based on a new type of adsorbent filling method. Materials, 2020, 13(1): 195
[115] Z. J. LI, M. Y. MA, S. S. ZHANG, et al. Efficiently removal of ciprofloxacin from aqueous solution by MIL-101 (Cr)-HSO3: the enhanced electrostatic interaction. Journal of Porous Materials, 2019, 27(1): 189-204
[116] Z. HASAN, J. W. JUN, S. H. JHUNG . Sulfonic acid-functionalized MIL-101(Cr): an efficient catalyst for esteri fication of oleic acid and vapor-phase dehydration of butanol. Chemical Engineering Journal, 2015, 278: 2 65-271
[117] J. Y. HOU, Y. LUAN, J. TANG, et al. Synthesis of UiO-66-NH2 derived heterogeneous copper (II) catalyst and study of its application in the selective aerobic oxidation of alcohols. Journal of Molecular Catalysis A: Ch emical, 2015, 407: 53-59
[118] H. MOLAVI, A. ESKANDARI, A. SHOJAEI, et al. Enhancing CO2/N2 adsorption selectivity via post-synthetic modification of NH2-UiO-66(Zr). Microporous and Mesoporous Materials, 2018, 257: 193-201
[119] C. Q. CHEN, D. Z. CHEN, S .S. XIE, et al. Adsorption behaviors of organic micropollutants on zirconium met al-organic framework UiO-66: analysis of surface interactions. ACS Applied Materials & Interfaces, 2017, 9 (46): 41043-41054
[120] S. HUANG, L. L. WAN, J. CARO. Microwave-assisted synthesis of well-shaped UiO-66- NH2 with high CO2 a dsorption capacity. Materials Research Bulletin, 2018, 98: 308-313
[121] Z. Q. LI, N. HORI, A. TAKEMURA. Synthesis and characterization of Cu-BTC metal-organic frameworks onto lignocellulosic fibers by layer-by-layer method in aqueous solution. Cellulose, 2019, 27(3): 1733-1744
[122] M. BILAL, M. BARANI, F. SABIR, et al. Nanomaterials for the treatment and diagnosis of Alzheimer's diseas e: an overview. NanoImpact, 2020, 20
[123] S. M. ASIL, J. AHLAWAT, G. G. BARROSO, et al. Nanomaterial based drug delivery systems for the treatme nt of neurodegenerative diseases. Biomaterials Science, 2020, 8(15): 4109-4128
[124] M. X. WU, Y. W. YANG. Metal-organic framework (MOF)-based drug/cargo delivery and cancer therapy. A dvanced Materials, 2017, 29(23):1606134